Text and references accompanying Nevada Bureau of Mines and Geology Map 154

STRATIGRAPHIC AND STRUCTURAL FRAMEWORK OF THE MEADVIEW NORTH QUADRANGLE, ARIZONA AND NEVADA

Mark A. Wallace[1], James E. Faulds[2], and Robert J. Brady[3]
[1]Department of Geology, University of Iowa, Iowa City, IA 52242
[2]Nevada Bureau of Mines and Geology, University of Nevada, Reno, NV 89557
[3]Department of Geology and Geophysics, University of Calgary, Calgary, AB, Canada, T2N 1N

REGIONAL SETTING

The Meadview North Quadrangle lies within the northeasternmost part of the Colorado River extensional corridor (Howard and John, 1987; Faulds and others, 1990), which is a 70- to 100-km wide region of moderately to highly extended crust between the Colorado Plateau on the east and Spring Mountains on the west. The quadrangle contains much of the town of Meadview, Arizona, as well as the southern part of the Grand Wash trough (including much of the Gregg Basin), southern part of Wheeler Ridge, and northern end of a mountain range informally referred to as the Lost Basin Range (after Theodore and others, 1987).

Both volcanism and large-magnitude east-west extension migrated north-northwestward across the northern Colorado River extensional corridor in Miocene time (e.g., Faulds and others, 1999, 2001a). Unlike most of the extensional corridor, however, volcanism within the vicinity of the quadrangle was minimal. Thus, sedimentary deposits (as opposed to volcanic strata) dominate the Grand Wash trough. East-west extension within the northern part of the corridor occurred between ~16 and 8 Ma (e.g., Anderson and others, 1972; Duebendorfer and Wallin, 1991; Beard, 1993, 1996; Faulds, 1993; Faulds and others, 1992, 1995, 2001a, 2002b; Price and Faulds, 1999; Harlan and others, 1998; Gans and Bohrson, 1998).

The Colorado River extensional corridor in the Lake Mead region is dominated by steeply east-tilted fault blocks that are bounded by major west-dipping normal faults (e.g., Brady and others, 2000). The west-dipping normal faults generally merge northward with the kinematically related right-lateral Las Vegas Valley shear zone and left-lateral Lake Mead fault system (Anderson, 1973; Duebendorfer and Wallin, 1991; Duebendorfer and Simpson, 1994; Beard, 1996; Duebendorfer and others, 1998), whereas to the south they generally die out in the Black Mountains accommodation zone, giving way to a system of east-dipping normal faults (Faulds and others, 1990, 2001a).

In contrast, the Colorado Plateau directly east of the corridor is virtually unextended and dominated by flat-lying Paleozoic strata (e.g., Lucchitta and others, 1986; Billingsley and others, 2004). Across much of central Arizona, a broad 100-km-wide transition zone separates the Colorado Plateau and Basin and Range province (Peirce, 1985). However, the transition zone in northwest Arizona is conspicuously narrow and essentially absent in the Lake Mead–Grand Canyon region.

The boundary between the Grand Canyon region of the Colorado Plateau and Colorado River extensional corridor in the Lake Mead region consists of a major west-dipping listric normal fault zone, the Grand Wash fault zone (Lucchitta, 1966, 1979). The Grand Wash fault zone bounds the Grand Wash trough on the east and is marked by the imposing fault-line escarpment of the Grand Wash Cliffs (figs. 1 and 2), which loom 800 m above the trough directly east of the quadrangle. The mouth of the Grand Canyon is carved into the Grand Wash Cliffs on the east side of the Grand Wash trough. Thus, the Colorado River flows directly from the Grand Canyon into the Grand Wash trough, where it dissects late Miocene to recent sedimentary and volcanic deposits in the basin.

The Grand Wash trough consists of at least two east-tilted half grabens, which are separated by Wheeler Ridge in the north and the Lost Basin Range in the south (fig. 1). The eastern half graben developed in the hanging wall of the west-dipping Grand Wash fault and is centered in the Grapevine Wash area. To the west, the Gregg Basin is a relatively narrow east-tilted half graben that lies in the hanging wall of the west-dipping Wheeler Ridge and Lost Basin Range faults. The Wheeler Ridge and Lost Basin Range faults probably represent splays of the Grand Wash fault zone. As Wheeler Ridge dies out to the north of Lake Mead, the two half grabens coalesce to form a large composite basin, at least at exposed levels. Dissection by the Colorado River and its tributaries has produced excellent exposures of the upper part of the Tertiary section in the Grand Wash trough.

Bohannon (1984) referred to the late Tertiary section in the Grand Wash trough as the "rocks of the Grand Wash trough," and we adopt this name as an informal group that encompasses the entire middle to late Miocene section deposited within the trough. This section includes, in ascending order, at least 250 m of middle to late Miocene fanglomerate, up to 120 m of sandstone and siltstone with locally interbedded gypsum, and as much as 300 m of late Miocene limestone (Longwell, 1936; Lucchitta, 1966;

Bohannon, 1984). The limestone in the Grand Wash trough has previously been referred to as the Hualapai Limestone and has been correlated with similar limestone elsewhere in the eastern Lake Mead region (Longwell, 1928, 1936; Lucchitta, 1966). The limestone has been interpreted as either marine (Blair, 1978; Blair and Armstrong, 1979) or nonmarine (Lucchitta, 1966; Faulds and others, 1997). The lower fanglomerate onlaps moderately to steeply (40–90°) east-tilted Paleozoic strata and Proterozoic gneiss at Wheeler Ridge and in the Lost Basin Range, as well as along the western margin of the trough in the South Virgin Mountains. The limestone onlaps subhorizontal Paleozoic strata along the Grand Wash Cliffs to the east. The late Tertiary section is generally tilted gently eastward (<10°). Most units thicken eastward toward the deeper parts of the half grabens.

The rocks of the Grand Wash trough are bracketed between ~15 and 7 Ma. The older age is based on a 15.3 Ma $^{40}Ar/^{39}Ar$ date on sanidine (table 1) from a rhyolite tuff near the base of the section on the west flank of Grapevine Mesa (Faulds and others, 2001b). The younger constraint is based on an 8.8 Ma basalt flow (Faulds and others, 2001b) intercalated with alluvial fan deposits shed from the Grand Wash Cliffs at Nevershine Mesa (Lucchitta and others, 1986) ~17 km northeast of the quadrangle. Furthermore, sanidine from a tephra (i.e., ash-fall tuff) intercalated in the upper part of the Hualapai Limestone at Grapevine Mesa yielded a maximum $^{40}Ar/^{39}Ar$ eruptive age of 7.43±0.22 Ma (table 1). Other workers have suggested deposition in the trough may have continued until 5–6 Ma (Blair and Armstrong, 1979; Lucchitta, 1989) on the basis of

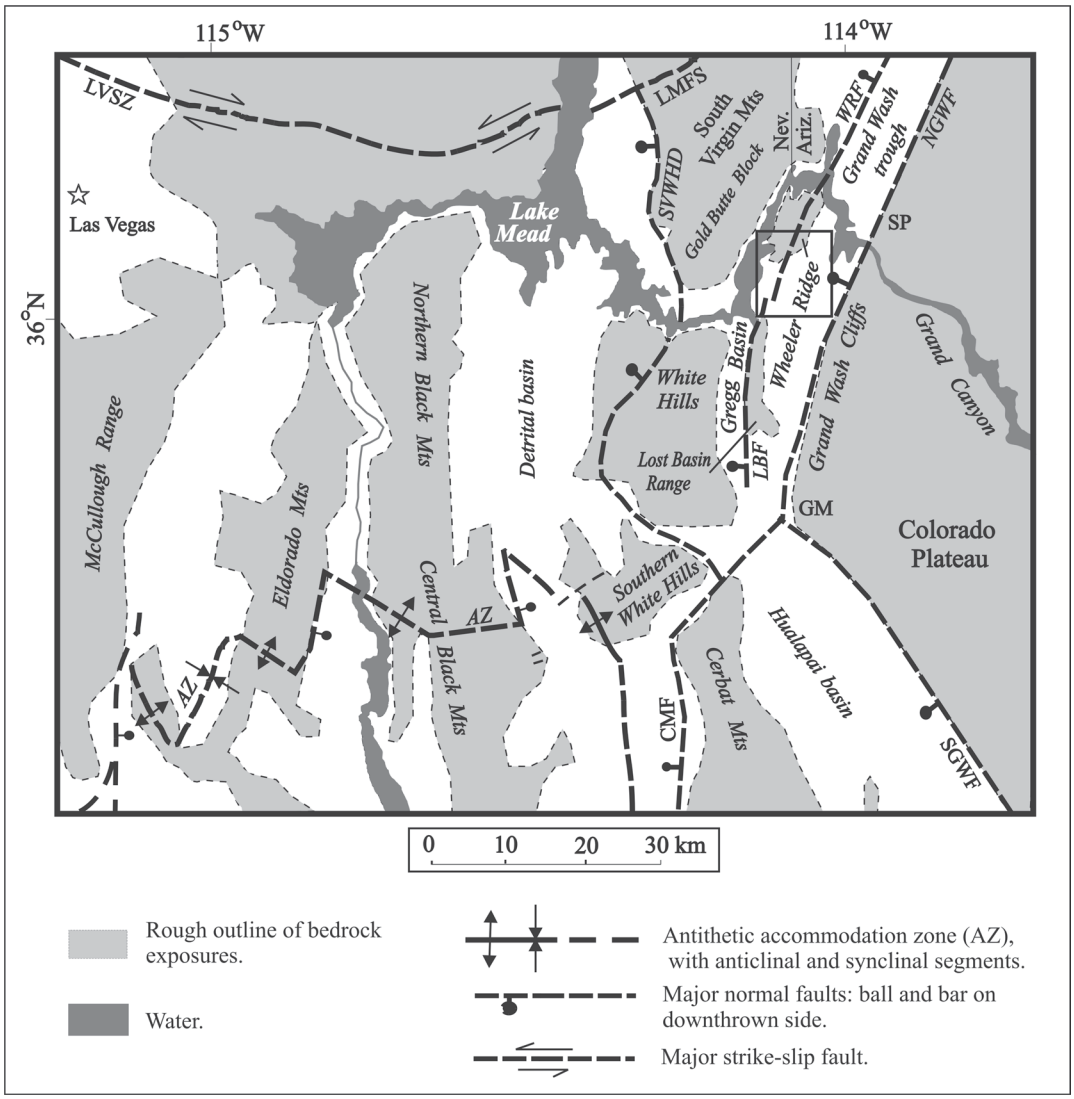

Figure 1. Generalized map of northwestern Arizona and southern Nevada, showing major physiographic features and structures. Box encompasses the Meadview North Quadrangle. The boundary between the Colorado Plateau and Basin and Range in this region is marked by the northern and southern Grand Wash fault zones. AZ, accommodation zone; CMF, Cerbat Mountains fault; GM, Garnet Mountain; LBF, Lost Basin Range fault; LMFS, Lake Mead fault system; LVSZ, Las Vegas Valley shear zone; NGWF, northern Grand Wash fault; SGWF, southern Grand Wash fault; SP, Snap Point; SVWHD, South Virgin-White Hills detachment fault; WRF, Wheeler Ridge fault.

correlating the Hualapai Limestone with limestone units in the Bouse Formation along the lower Colorado River to the southwest. A 6.0 Ma tephra within the Hualapai Limestone to the west of the Grand Wash trough supports this premise (Spencer and others, 2001).

The rocks of the Grand Wash trough have significant paleogeographic implications (Lucchitta, 1966, 1979). For example, the timing of possible uplift of the Colorado Plateau during late Cenozoic time (McKee and McKee, 1972) has been extrapolated from studies of basinal sedimentary deposits within the Grand Wash trough and elsewhere within the lower Colorado River region (Lucchitta, 1979). The Hualapai Limestone is particularly important.

Lucchitta (1966) characterized the limestone as lacustrine based on facies relationships with detrital rocks in the Grand Wash trough. Blair (1978), Blair and Armstrong

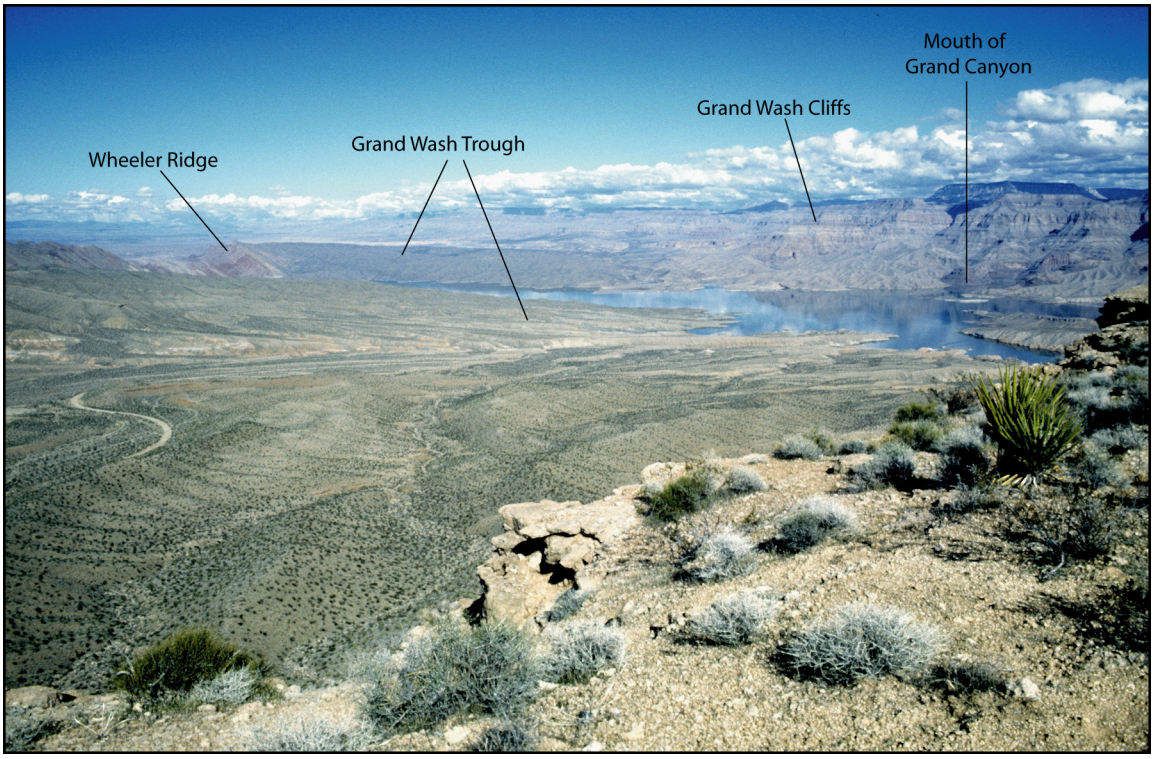

Figure 2. View looking north at Grand Wash trough, Grand Wash Cliffs, and Wheeler Ridge from Airport Point at the north end of Grapevine Mesa.

Table 1. $^{40}Ar/^{39}Ar$ **Isotopic Age Determinations, Southern Grand Wash Trough, Northwest Arizona**

Sample #	Map Label	Location Lat (N)	Location Long (W)	Tilt Magnitude	Rock unit/Sample area	Material Dated or Correlated	Apparent Age (Ma)	Source
JF-97-76	A	36°06'53"	114°06'41"	0°	Tbsp-Sandy Point	Groundmass	4.41±0.03	USGS
MW-98-36	B	36°00'39"	114°02'55"	~5° East	Ash-fall tuff-near Meadview	Sanidine	7.43±0.22*	NM
MW-97-18	C	36°06'00"	114°02'24"	~4° East	Ttgw within Tsgw -Airport Point	Glass-geochemical correlation	10.94±0.03	UU
JF-97-144	D	36°03'19"	114°00'53"	~4° East	Ttgw-Grapevine Wash	Glass-geochemical correlation	10.94±0.03	UU
JF-97-144	E	36°03'19"	114°00'53"	~4° East	Ttgw-Grapevine Wash	Sanidine	11.08±0.27	NM
JF-98-155	F	36°06'54"	114°00'01"	~5° East	Ttpf-Pearce Ferry	Sanidine	13.11±0.08*	NM
JF-98-308	G	36°03'03"	114°05'32"	30° East	Tts-Nonwelded tuff West flank, Grapevine Mesa	Sanidine	15.29±0.07	NM

Sample locations are shown on map by letters designated in map symbol column. For rock type: Tbsp, basalt of Sandy Point; Ttgw, tephra in Grapevine Wash area; Ttpf, tephra in Pearce Ferry area. *Maximum eruptive age. For source: NM, laser-fusion (sanidine) or weighted mean plateau (groundmass) ages from New Mexico Bureau of Mines; USGS, weighted mean plateau ages from M. Kunk, U.S. Geological Survey (Denver); UU, glass geochemistry correlation (tephrachronology) from M. Perkins, University of Utah.

(1979), and Bradbury and Blair (1979) used fossil assemblages, petrography, and $\delta^{13}C$ isotopic chemistry to interpret the Hualapai Limestone as marine-estuarine. They further concluded that the Hualapai Limestone marked the northern extent of an ancestral Gulf of California. This inference was based on the assumption that the Hualapai Limestone and the presumably marine or estuarine Bouse Formation (Metzger, 1968; Smith, 1970; Buising, 1990) in the lower Colorado River region were similar in age and deposited at approximately the same elevations (sea level or below), because no significant late Miocene to recent faulting was documented within or between the two regions (Lucchitta, 1979). These deposits were therefore used to support 400–900 m of Pliocene-Quaternary uplift of the Colorado River extensional corridor and western part of the Colorado Plateau (Lucchitta, 1979, 1998). This uplift presumably induced rapid downcutting of the Grand Canyon by the Colorado River since 6 Ma (Lucchitta, 1979, 1989).

Several recent studies, however, have raised serious questions about these interpretations. For example, Spencer and Patchett (1997) concluded on the basis of $^{87}Sr/^{86}Sr$ isotopic evidence that carbonates within the late Miocene to Pliocene Bouse Formation in the lower Colorado River region and the Hualapai Limestone near Temple Bar are lacustrine in origin. Furthermore, Faulds and others (1997, 2001c) and Wallace (1999) marshaled evidence from fossil assemblages, petrography, and $\delta^{13}C$–$\delta^{18}O$ and $\delta^{34}S$ isotopic geochemistry in support of a nonmarine (lacustrine) origin for both the Hualapai Limestone and a 2.5 km-thick middle to late Miocene salt deposit in the nearby Hualapai basin (fig. 1). If not marine or estuarine, the carbonate deposits within the Lake Mead and lower Colorado River regions cannot be used as evidence to support: 1) late Miocene to recent uplift of the southwestern Colorado Plateau; 2) the northern extent of the ancestral Gulf of California; and 3) rapid downcutting of the Grand Canyon since 6 Ma. Thus, the nature of Colorado Plateau uplift, evolution of the boundary between the Colorado Plateau and Basin and Range province, and development of the Colorado River and Grand Canyon are all in dispute. The Cenozoic sedimentary rocks within the Meadview North Quadrangle, particularly the Hualapai Limestone, are therefore critical for deciphering the late Cenozoic structural and paleogeographic evolution of the southwestern Cordillera.

STRATIGRAPHY

The major lithologies in the Grand Wash trough are here described in ascending order, with an emphasis on Tertiary deposits including the limestone, sandstone-siltstone, and fanglomerate facies in the Grand Wash trough. A large paleocanyon carved into the Paleozoic strata of Wheeler Ridge is also described. The map explanation provides more complete descriptions of individual rock units.

Proterozoic Rocks

Proterozoic rocks crop out in the western part of the quadrangle in both the Wheeler Ridge area and northern Lost Basin Range. They consist of strongly foliated Early Proterozoic orthogneiss and paragneiss and Middle Proterozoic diabase and gabbro. U-Pb dating in nearby areas indicates that the gneisses are ~1.69 Ga (Karlstrom and Bowring, 1991) and are probably correlative with other 1.6 Ga gneisses and granites in the region (e.g., Wasserburg and Lanphere, 1965; Albin and Karlstrom, 1991; Fryxell and others, 1992). In the South Virgin Mountains 12–15 km west of the quadrangle, a thick crustal section, which includes a large body of 1.4 Ga Gold Butte rapakivi granite, is exposed in the steeply east-tilted Gold Butte block (Wasserburg and Lanphere, 1965; Silver and others, 1977; Fryxell and others, 1992; Brady, 1998; Howard and others, 2003). The Proterozoic rocks in the Lost Basin Range and Gold Butte block provided a major source of clastic material that was shed eastward and northward during Miocene time into the Grand Wash trough (Lucchitta, 1966; Lucchitta and Young, 1986).

Paleozoic Strata

Paleozoic rocks form the subhorizontal strata in the Grand Wash Cliffs directly east of the Grand Wash trough and moderately to steeply (40–90°+) east-tilted strata at Wheeler Ridge within the trough (figs. 2 and 3). The Paleozoic section rests nonconformably on the Proterozoic gneiss and granitoids. Limestone and dolomite dominate the Paleozoic strata, but clastic units are found in the basal part of the Cambrian and in the Pennsylvanian sections.

As a result of gentle regional northeast-tilting and erosional beveling in Cretaceous to early Tertiary time (Lucchitta and Young, 1986), progressively older units crop out to the south within the Grand Wash Cliffs. For example, Mississippian through Permian units dominate surface exposures north of the Grand Canyon, whereas Cambrian through Mississippian units prevail to the south. Similarly, on Wheeler Ridge, only Cambrian through Pennsylvanian units are exposed in the Meadview North Quadrangle, whereas Cambrian through Permian units crop out to the north of Lake Mead (Lucchitta and Young, 1986).

Wheeler Ridge Paleocanyon

The moderately to steeply east-tilted Paleozoic strata on Wheeler Ridge are cut by an at least 200 m-deep early Tertiary or middle Miocene paleocanyon, here referred to as the Wheeler Ridge paleocanyon. The paleocanyon is marked by a 3.5 km-wide gap in exposures of Paleozoic strata extending southward from the vicinity of the South Cove road (fig. 4), as first noted by Longwell (1936). The paleocanyon may trend east-southeast and connect westward with a paleocanyon mapped by K. Howard (personal commun., 1998) in the Hiller Mountains (southern part of the South Virgin Mountains). Middle to late Miocene

fanglomerates and megabreccia deposits, largely derived from the South Virgin Mountains (Lucchitta, 1966), fill the paleocanyon.

Several scenarios are possible for the age and origin of the Wheeler Ridge paleocanyon. These include: 1) excavation during middle Miocene time contemporaneous with movement on the Grand Wash fault, fault-block tilting, and development of the Grand Wash trough; and 2) excavation during early Tertiary time by a northeast-flowing consequent drainage, similar to those documented ~65 to 90 km to the southeast on the Hualapai Plateau (Young, 1970, 1979). We favor the former explanation, because the southern margin of the paleocanyon truncates west-dipping normal faults that cut Paleozoic strata and are presumably middle Miocene in age.

Tertiary Strata: Rocks of the Grand Wash Trough

All Tertiary strata deposited within the Grand Wash trough are grouped into the rocks of the Grand Wash trough (after Bohannon, 1984). These strata primarily consist of basinal sedimentary rocks intercalated locally with thin volcanic units (Lucchitta, 1966). The letters shown in parentheses in this section correspond to the map labels for individual units. The Tertiary units within the quadrangle overlie Paleozoic strata in angular unconformity. Fanglomerate (Tcg and Tcp) dominates the lower exposed section within the Grand Wash trough. Thin tuffs and tuffaceous sediments (Tts) are intercalated with the lowermost part of the fanglomerate along the west flank of Grapevine Mesa near the north end of the Lost Basin Range. Several megabreccia deposits (Tbs, Tbx, Tbp, and Tbpx) indicative of large rock avalanches are also interbedded within the fanglomerate. A sandstone and siltstone unit (Tsgw and Tsgb) with an exposed thickness of 2 to 120 m overlies and interfingers with the fanglomerate. The overall thickness of the sandstone-siltstone unit is probably much greater than 120 m. A 20- to 30-m-thick section of primary gypsum and several thin lenses of secondary gypsum are intercalated within the sandstone-siltstone unit. Overlying and interfingering with the sandstone-siltstone unit is the Hualapai Limestone (Thgw, Thgb), which is as much as 300 and 170 m thick in the Grapevine Wash area and Gregg Basin, respectively.

Older Tuffaceous Sediments (Tts)

The Tts unit is one of the oldest exposed Tertiary units within the quadrangle. It consists of a thin section (< 30 m) of interbedded nonwelded tuff, tuffaceous sedimentary rock, and volcaniclastic sandstone and is intercalated with the lower part of the fanglomerate section. Tts crops out only as small west-dipping, hanging-wall slivers dragged against the southernmost part of the Wheeler Ridge fault (see geologic map). Sanidine from a nonwelded tuff within Tts has yielded an $^{40}Ar/^{39}Ar$ age of 15.29±0.07 Ma (table 1).

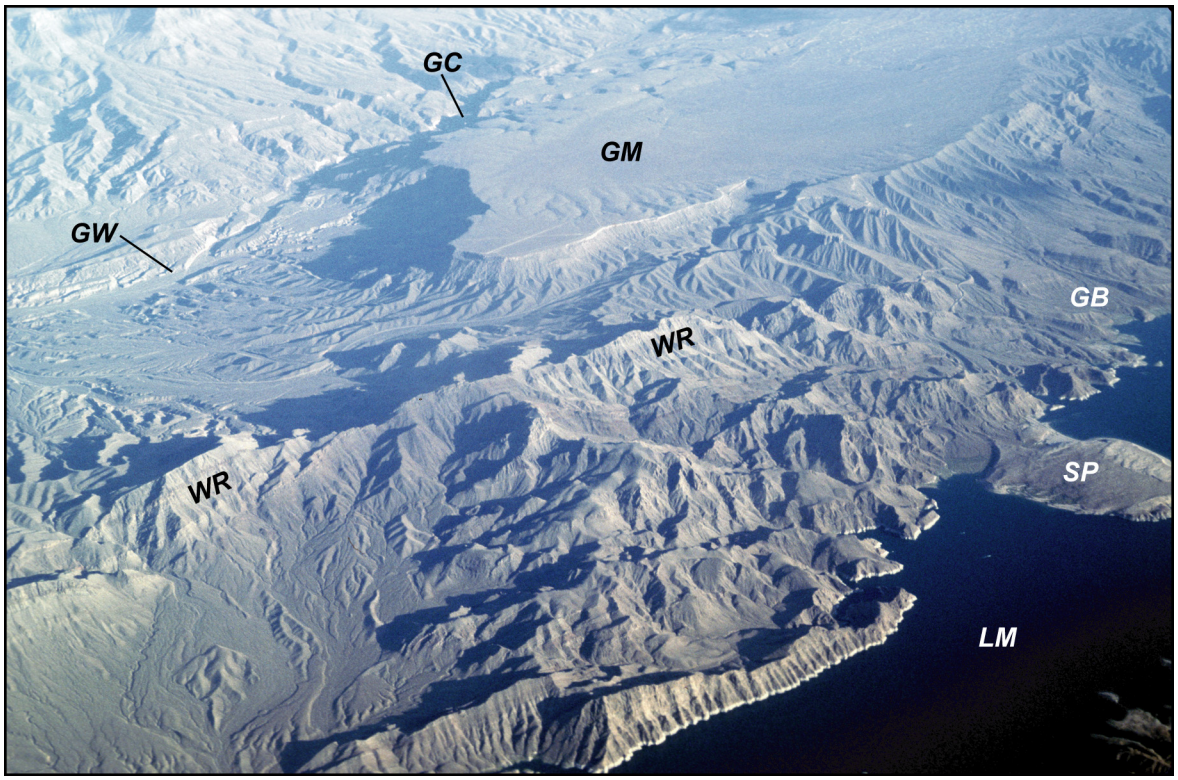

Figure 3. Aerial view of much of the Meadview North Quadrangle, including Grapevine Mesa (GM, which is capped by the Hualapai Limestone), Grapevine Canyon (GC), Grapevine Wash (GW), Gregg Basin (GB), Lake Mead (LM), Sandy Point (SP), and Wheeler Ridge (WR).

Fanglomerate (Tcg and Tcp)

Conglomerate (Tcg and Tcp) is the thickest exposed unit within the Grand Wash trough. Easterly dips in the 250-m-thick section of conglomerate on the west flank of Grapevine Mesa decrease upward from ~25° to ~4°. The unit locally contains ~0.5-m-thick lenses of sandstone. The overlying sandstone-siltstone and limestone units grade into and interfinger with the conglomerate. $^{40}Ar/^{39}Ar$ dates and geochemical correlations of tuffs in the Tts and sandstone-siltstone units (Tsgw) bracket the age of the conglomerate between ~15.3 and 11 Ma.

On the basis of clast lithology, two types of conglomerate were distinguished in the Grand Wash trough. Conglomerate to the west of Grapevine Wash (Tcg) is generally dominated by Proterozoic clasts, including the distinctive ~1.4 Ga megacrystic rapakivi-type (e.g., Volborth, 1962) Gold Butte Granite exposed in the South Virgin Mountains to the west and Early Proterozoic gneiss exposed in both the South Virgin Mountains and Lost Basin Range. In contrast, on the east side of Grapevine Wash, clast lithologies are generally dominated by Paleozoic limestones and dolostones derived from the Grand Wash Cliffs to the east (Tcp). Paleozoic-clast conglomerate is also locally found proximal to the Paleozoic outcrops of Wheeler Ridge (Lucchitta, 1966).

The poor sorting, angularity and size of clasts, both matrix- and clast-supported beds, and intercalated lenses of sandstone suggest that the conglomerate originated as debris-flow and sheetflood deposits on alluvial fans (e.g., Nilsen and Moore, 1984; Blatt and others, 1980). In addition, fan-shaped geometries are observed just north of Airport Point and along the eastern flank of Wheeler Ridge (e.g., Lucchitta and Young, 1986).

These fanglomerates were shed from the surrounding highlands, including the Grand Wash Cliffs, South Virgin Mountains, and Lost Basin Range. The Paleozoic-clast conglomerate (Tcp) east of Grapevine Wash was derived from the Grand Wash Cliffs, as the unit thickens and clast size increases toward the cliffs. The Proterozoic-clast conglomerate (Tcg) in the Wheeler Ridge area and along the west flank of Grapevine Mesa contains large boulders of 1.4 Ga Gold Butte Granite derived from the South Virgin Mountains to the west (Lucchitta, 1966).

Rock Avalanche Deposits (Tbx, Tbp, Tbpx, Tbs)

Four types of sedimentary breccia and megabreccia are interbedded with the fanglomerate facies on the west flank of Grapevine Mesa primarily within the Wheeler Ridge paleocanyon. Crackle and jigsaw breccia (Yarnold and Lombard, 1989) are divided into three map units on the basis of clast composition: 1) granitic- and gneissic-clast breccia (Tbx), which is the most common type of megabreccia; 2) Paleozoic limestone- and dolostone-clast breccia (Tbp); and (3) a mix of the previous two types (Tbpx). The texture, small amount of matrix, and angularity of both small and large fragments indicate that these breccia deposits originated as large rock avalanche deposits, which may have been triggered by paleo-earthquakes associated with movement on the Grand Wash or related fault zones. The granitic- and gneissic-clast breccia (Tbx) was most likely derived from the South Virgin Mountains now ~11 km to the west, which exposes large tracts of gneiss and megacrystic Gold Butte Granite (e.g., Howard and others, 2003). Large rock avalanche deposits have been documented traveling up to 15 km from their source (Harrison and Falcon, 1937; Pierson and Costa, 1987). Breccia units containing clasts of Paleozoic limestone and dolostone (Tbp) were probably derived from the nearby walls of the Wheeler Ridge paleocanyon. The rock avalanche deposits are primarily intercalated within the lower part of the exposed fanglomerate section and, thus, are probably ~15 Ma.

Sandstone-Siltstone and Gypsum units (Tsgw, Tggw, Tsgb)

The sandstone-siltstone units of the Grand Wash trough interfinger with and grade into both the overlying limestone and underlying fanglomerate facies. In the lower Grapevine Wash area of the Grand Wash trough (fig. 4), the sandstone-siltstone unit envelops a lens of primary silty gypsum (Tggw), which reaches an exposed thickness of ~20 m. The exposed thicknesses of the sandstone-siltstone facies in the Grapevine Wash area and Gregg Basin are 120 and 95 m, respectively (Longwell, 1936). We speculate that the unexposed thickness of these deposits may be much greater (e.g., cross section A–A′).

The depositional environment of the sandstone-siltstone facies was probably a highly evaporative interior continental playa, as evidenced by the intercalated gypsum, thin bedding, and mudcracks. The lack of fluvial textures, such as cross-beds or ripple marks, local abundance of gypsum rinds, interfingering and bordering fanglomerate facies, and 20-m-thick interbedded gypsum unit (Tggw) appear to rule out any rigorous and/or constant through-going axial drainage.

The fanglomerate and sandstone-siltstone facies are probably related, but the grayish-brown matrix in the Proterozoic-clast fanglomerate contrasts with the reddish sandstone and siltstone. This suggests that at least two different source areas fed sediment into the Grand Wash trough. The Proterozoic-clast conglomerate was probably derived primarily from the crystalline terranes of the South Virgin Mountains and possibly Lost Basin Range, whereas the sandstone-siltstone facies may have been largely derived from non-resistant Pennsylvanian-Permian redbeds (e.g., Hermit and Supai Formations) on the Colorado Plateau and/or to the north of the Grand Wash trough.

The exposed part of the sandstone-siltstone facies within the Meadview North Quadrangle is bracketed between ~13 and 11 Ma. Nonwelded tuffs in the lower part of the exposed section in the Pearce Ferry area have yielded fission-track ages ranging from 10.8±0.8 to 11.6±1.2 Ma (Bohannon, 1984) and a maximum $^{40}Ar/^{39}Ar$ age on sanidine of 13.11±0.08 Ma, whereas a tephra in the upper part of the section in Grapevine Wash geochemically correlates with a 10.94±0.03 Ma tuff (table 1). At Nevershine Mesa north of

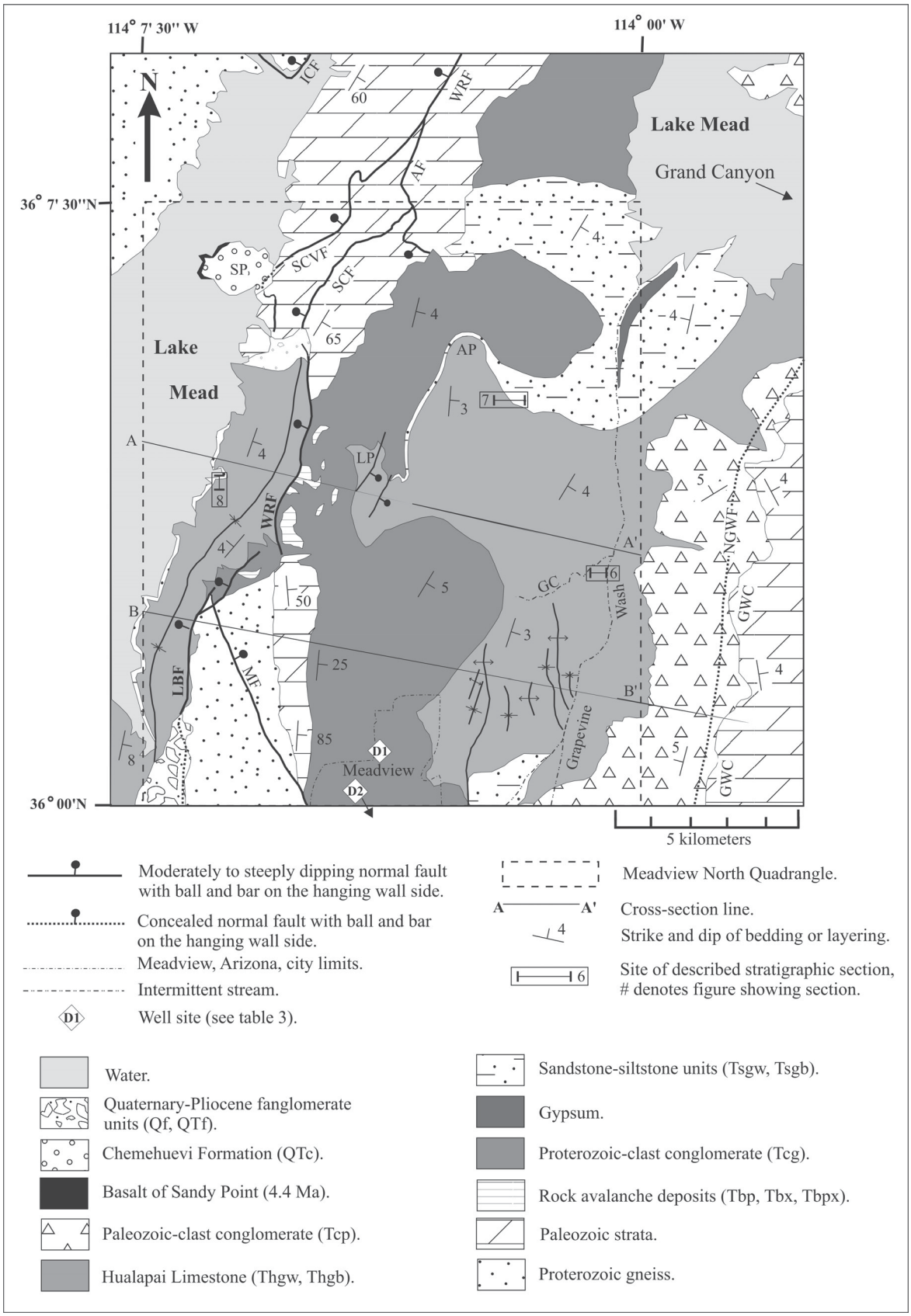

Figure 4. Generalized geologic map of the Meadview area in the Grand Wash trough. Refer to map for explanation of geologic units. AF, Airport fault; AP, Airport Point; GC, Grapevine Canyon; GWC, Grand Wash Cliffs; ICF, Iceberg Canyon fault; LBF, Lost Basin Range fault; LP, Lookout Point; MF, Meadview fault; NGWF, northern Grand Wash fault; SCF, Sheep Canyon fault; SCVF, South Cove fault; SP, Sandy Point; WRF, Wheeler Ridge fault.

Lake Mead, a basalt flow intercalated with alluvial fan deposits that overlie the sandstone-siltstone facies (Lucchitta and others, 1986) has yielded an 8.8 Ma $^{40}Ar/^{39}Ar$ age (Faulds and others, 2001b). Thus, the sandstone-siltstone facies may be as young as ~9 Ma in parts of the Grand Wash trough. The age of the exposed gypsum facies is probably ~11 Ma, because it lies only a few tens of meters down section from the 10.94 Ma tephra.

Tephras

The rocks of the Grand Wash trough contain several thin ash-fall tuffs or tephras. Although several tephras or tuffaceous "zones" ranging from 0.25 to 2 m were mapped (Ttu), many additional thinner (<20 cm thick) ash-fall deposits crop out within the limestone and sandstone-siltstone units but are commonly reworked and/or altered to clay. Two of the more prominent tephras crop out at Pearce Ferry and in Grapevine Wash.

The tephra at Pearce Ferry is intercalated within the sandstone-siltstone unit near the level of Lake Mead (~366 m elevation) and crops out as a conspicuous white band in the low cliffs along Lake Mead in the Pearce Ferry area (fig. 5). Set in a matrix of volcanic glass shards, very fine grained phenocrysts compose ~5% of the rock and include quartz, plagioclase, sanidine, and biotite. A 13.11±0.08 Ma $^{40}Ar/^{39}Ar$ date (maximum age) was obtained on sanidine (table 1) from the tephra at Pearce Ferry.

The tephra in Grapevine Wash has a distinctive light gray color and is as much as 2 m thick. Intercalated either within the lowermost part of the Hualapai Limestone or uppermost part of the sandstone-siltstone facies, it dips gently east and therefore crops out ~150 m higher in elevation just north of Airport Point compared to its exposure in Grapevine Wash (see geologic map). This tephra locally contains moderately indurated lenses up to ~5 cm thick in its upper 0.5 m in the Airport Point area. It is composed of a volcanic glass matrix with ~1–2% very fine-grained phenocrysts including quartz, titanomagnetite, plagioclase, sanidine, and biotite. The tephra in Grapevine Wash yielded an $^{40}Ar/^{39}Ar$ age on sanidine of 11.08±0.27 Ma and has been geochemically correlated (two samples) with a 10.94±0.03 Ma tuff (Perkins and others, 1998; Perkins and Nash, 2002) derived from the Bruneau-Jarbidge volcanic field in the Trapper Creek area of southernmost Idaho in the Snake River Plain volcanic province (M. Perkins, written commun., 1998). Two ash-fall deposits lying stratigraphically between the tephras at Pearce Ferry and in Grapevine Wash have given zircon fission-track ages of 10.8±0.8 Ma to 11.6±1.2 Ma (Bohannon, 1984).

Hualapai Limestone (Thgw, Thgb)

The Hualapai Limestone in the Grapevine Wash area (Thgw) is similar in lithology, texture, and stratigraphic position to that in the Gregg Basin (Thgb). Both interfinger with and overlie the sandstone-siltstone facies of their respective basins. However, because they may have been partly deposited in discrete basins, the limestone units in each area are described as separate map units. Four stratigraphic sections of the Hualapai Limestone were measured and described in detail by Wallace (1999) (figs. 6, 7, 8). These show the relative abundance of sandstone and siltstone interbeds as well as some differences between the limestone units in the Grapevine Wash area and Gregg Basin.

Petrographic analysis indicates that the limestone in both basins is dominantly pelmicrite and rarely contains fossils (Wallace, 1999). Slight differences in general texture and composition distinguish the limestones of each basin. However, the distinguishing characteristics of one basin may be locally common in the other basin.

In the Grapevine Wash area (figs. 3, 4, and 6), the limestone consists of a relatively thick section of wavy laminated, white to pinkish tan, vuggy pelleted packstone, wackestone, and calcareous mudstone (Wallace, 1999). In the central part of Grapevine Wash (figs. 4 and 6), the unit

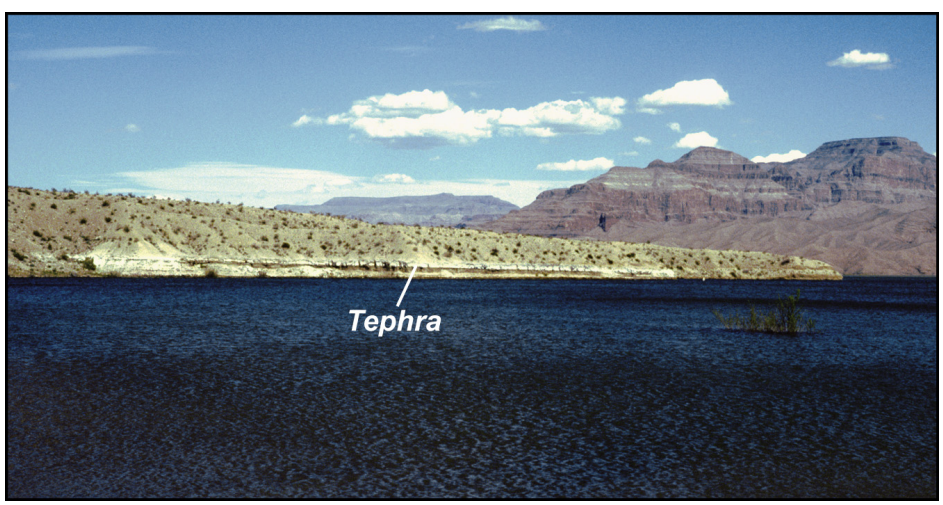

Figure 5. Looking north at 13.1 Ma tephra along Lake Mead in the Pearce Ferry area. The 13.1 Ma date is a maximum eruptive age.

is massively bedded, contains rare siltstone laminations, and is as much as 300 m thick. Along the eastern margin of exposure, the limestone grades into reddish-brown or gray clast-supported conglomerate (Tcp) containing clasts of Paleozoic limestone in a medium to coarse-grained, calcite-cemented sandy matrix.

In the Gregg Basin, the Hualapai Limestone has generally undergone less neomorphism and contains only a minor amount of wavy laminations (or 'eggshell' texture). The most distinguishing characteristic of the limestone in the Gregg Basin, however, is the relatively greater abundance of poorly indurated sandstone, siltstone, and sub-rounded

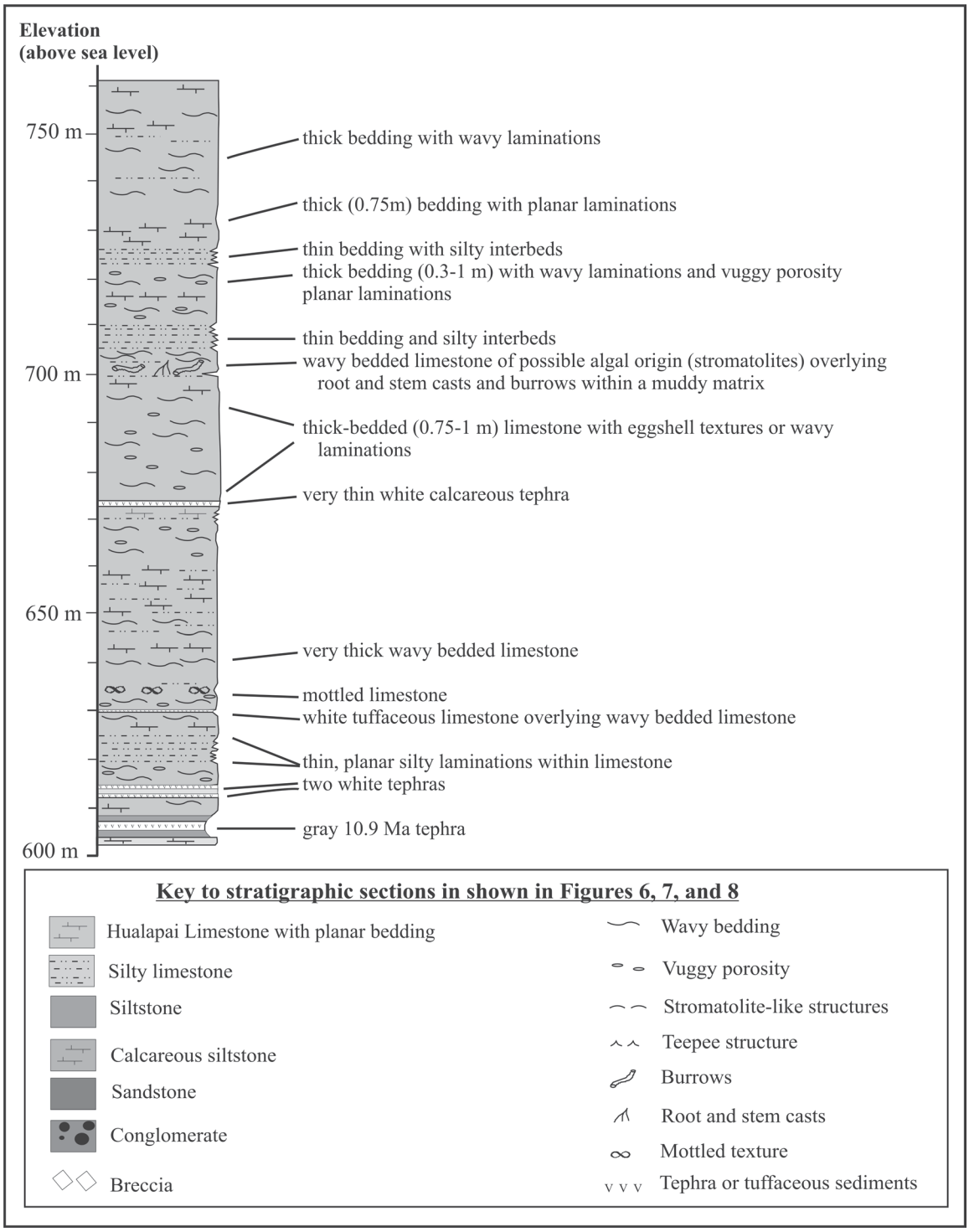

Figure 6. Generalized stratigraphic section of Hualapai Limestone in Grapevine Wash (Thgw) at 36°02'40"N, 114°00'59"W and key to figures 6, 7, and 8. See figure 4 for location of sections and text for description of units. Note the thick limestone (Thgw) and relatively small amount of intercalated sandstone and siltstone.

to angular pebble conglomerate interbeds, which collectively compose up to 50% of a given section in some areas (figs. 6, 7, and 8). Locally within the Gregg Basin, conglomerate interbeds derived from the nearby Paleozoic limestone and dolostone on Wheeler Ridge pinch out to the west, as first noted by Longwell (1936). Only one prominent interbedded tephra (unmapped) was found within the exposed section in the Gregg Basin and is located in the upper part of the limestone on the east side of Hualapai Wash (Wallace, 1999). This also distinguishes it from limestone in the Grapevine Wash area, where several thin tuffs are intercalated in the upper and lower parts of that section.

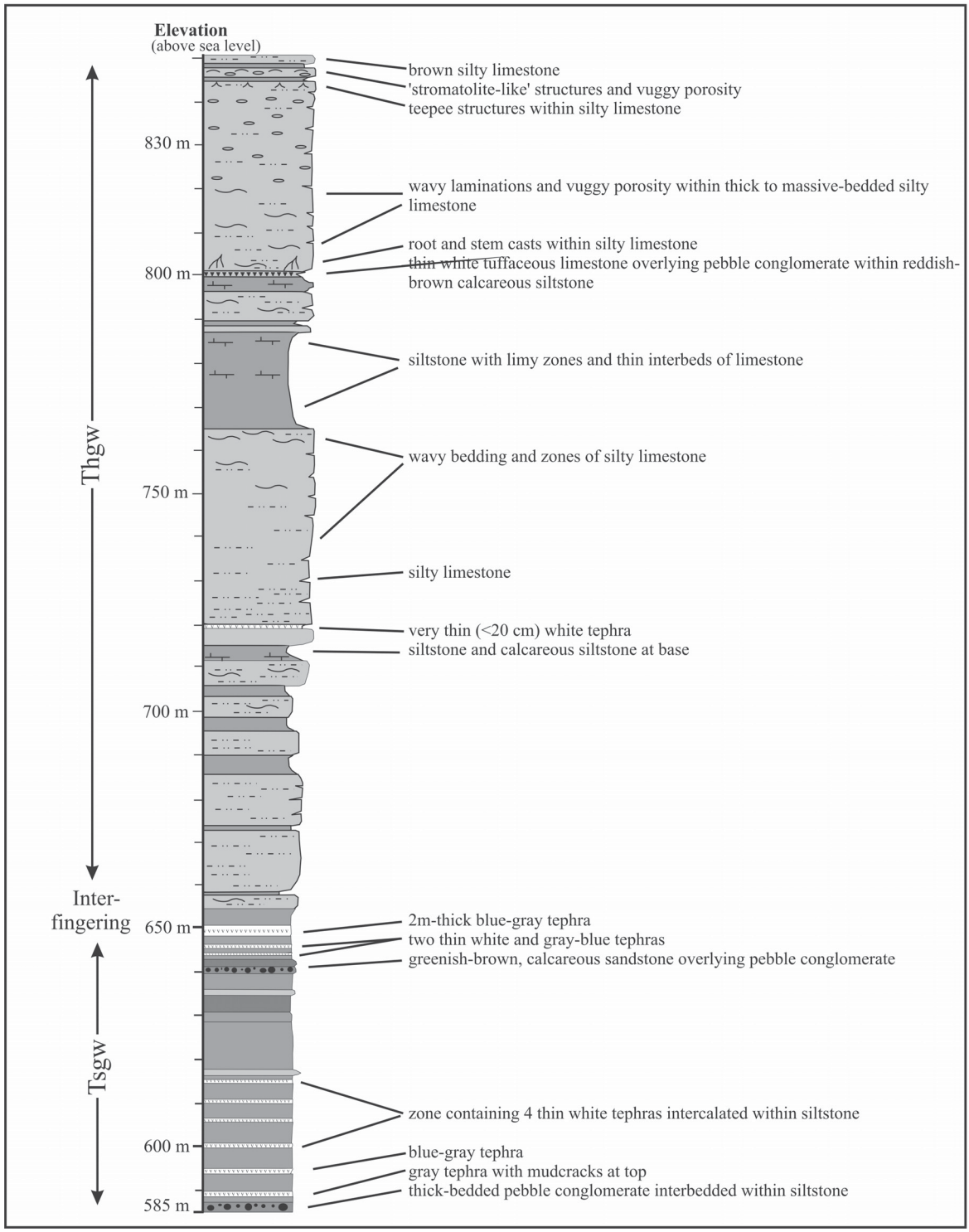

Figure 7. Generalized stratigraphic section measured southeast of Airport Point roughly at 36°04'54"N, 114 °02'03"W (see fig. 4 for location). Sandstone and siltstone (Tsgw) grade upward and interfinger with limestone (Thgw). See figure 6 for key and map explanation for descriptions of units.

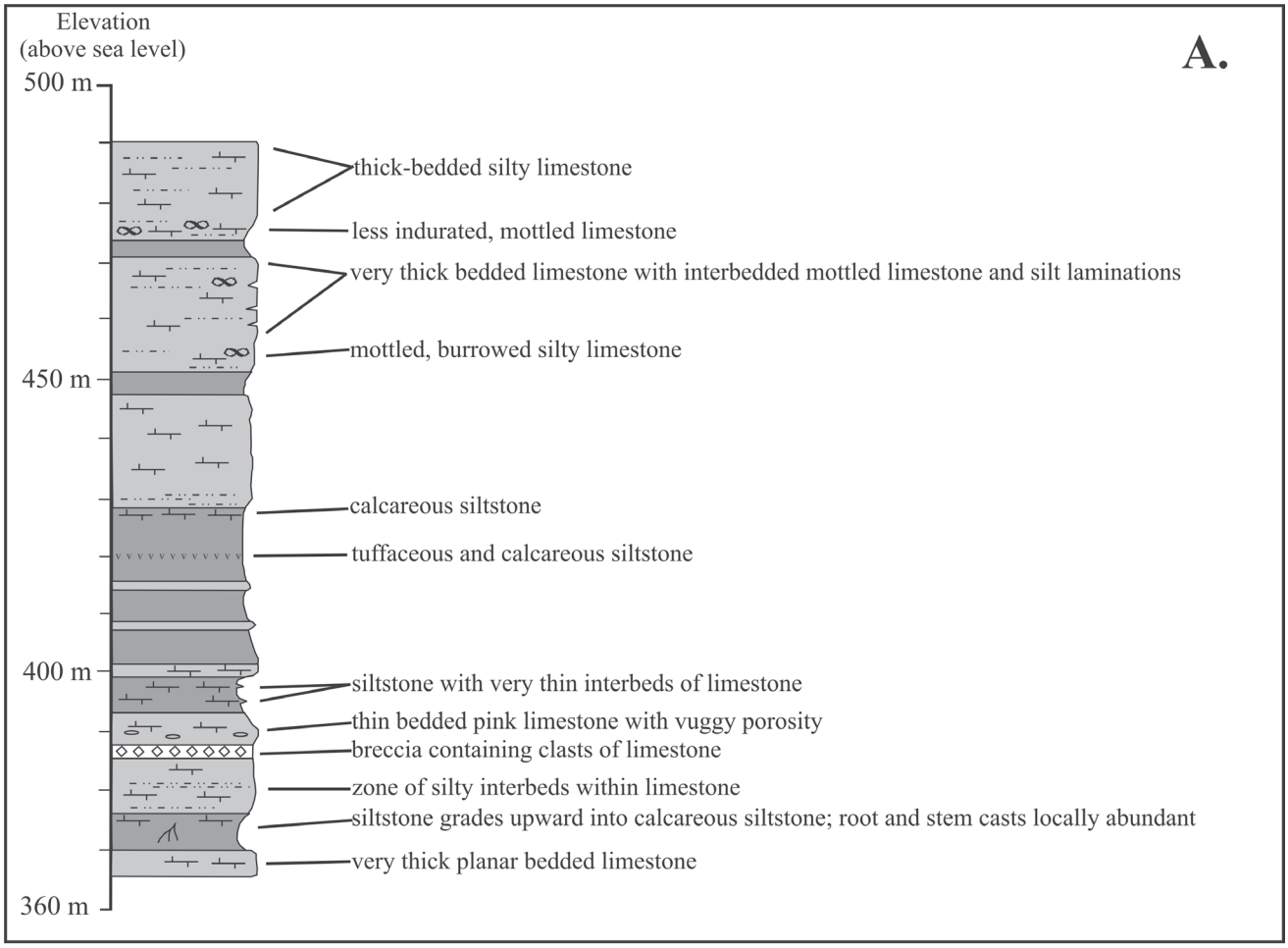

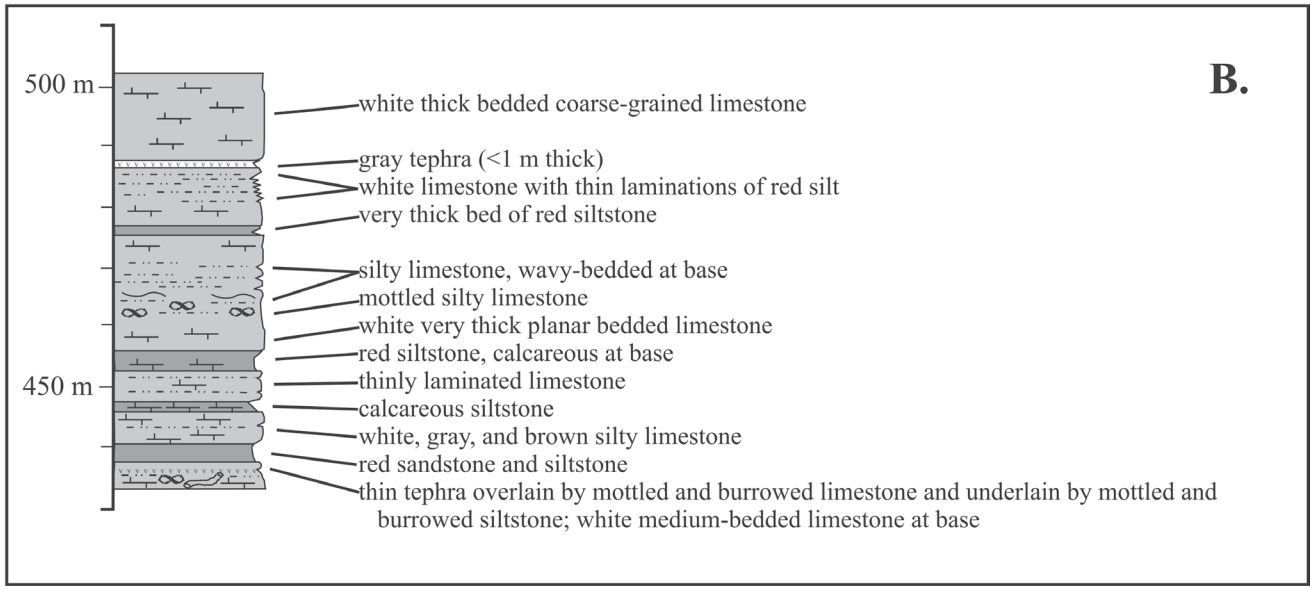

Figure 8. Generalized stratigraphic sections of Hualapai Limestone in Gregg Basin (Thgb) measured near Wagon Trail Bay (A) and Hualapai Wash (B) at 36°03'59"N, 114°05'51"W and 35°59'13"N, 114°8'19"W, respectively. See figure 4 for location of (A) and map explanation for descriptions of units. (B) is located ~3 km west-southwest of the Meadview North Quadrangle. Note the relative abundance of siltstone (Tsgb) interbedded within the limestone here (Thgb) as compared to that in the Hualapai Limestone in the Grapevine Wash area (Thgw, fig. 6). The sections from the Gregg Basin (both A and B) and the section shown in figure 6 from the Grapevine Wash area are all located in the apparent depocenters of their respective basins.

Although offset by ~275 m on the west-dipping Wheeler Ridge fault, the uppermost limestone beds within the Gregg Basin probably correlate with those in the Grapevine Wash area and represent a time when the two basins had coalesced. Siltstone interbeds are more common in the upper 20 m of limestone within the Gregg Basin than that on the rim of Grapevine Mesa, where the upper 20 m are composed of relatively continuous limestone deposited on fanglomerate. An ~1-m-thick reddish calcite-cemented pebble conglomerate is, however, interbedded within the upper 20 m of both sections and is exposed along both the South Cove Road in the Gregg Basin and western edge of Grapevine Mesa at Lookout Point.

In contrast to the interpretation of Blair and Armstrong (1979), petrographic analysis revealed no indication of a marine or estuarine setting (Wallace, 1999; Faulds and others, 2001c). Fossils include only ostracods, green algae (including charophytes), algal mats, oncolites, and possible stromatolites in a typically pelleted micrite substrate. None of the fossils are diagnostically marine (e.g., Heckel, 1972). Ostracods are highly tolerant organisms that can live in extreme conditions that include fresh to hypersaline and clear to sediment-loaded water and hard to mobile substrate. Blue-green and green algae can also live in several environments but are constrained to the photic zone. In addition, charophytes need clear, fresh water to survive (Heckel, 1972). Furthermore, locally abundant flowstone indicates a constant source of fresh water that is super-saturated with respect to calcium carbonate, either issuing from springs or perennial streams.

$\delta^{13}C$ and $\delta^{18}O$ isotopic analyses were obtained at the University of Michigan Stable Isotope Laboratory from 22 samples of the Hualapai Limestone in the quadrangle. All analyses are reported relative to the PDB standard (based on belemnites from the Cretaceous Peedee Formation) and precision is better than 0.1% for both ^{13}C and ^{18}O. The data (table 2) show consistent values with minimum scatter that can be confidently characterized with respect to other carbonates from various regions around the world.

With only one exception, very low $\delta^{18}O$ values and highly variable $\delta^{13}C$ (table 2) characterize the limestone, both of which are indicative of a nonmarine setting (e.g., Talbot and Kelts, 1990). In addition, the 5 to 6 ‰ variation in $\delta^{18}O$ values is consistent with those of other lacustrine carbonates reported from various regions of the world (Stuiver, 1970; Stiller and Hutchinson, 1980; Spencer and others, 1984; McKenzie, 1985; Hillaire-Marcel and Casanova, 1987; Halfman and others, 1989; Talbot and Kelts, 1990; Tenzer and others, 1997). Based on the present-day regional distribution of $\delta^{18}O$ in meteoric waters (Sheppard and others, 1969; Drever, 1997) and the latitude of the Grand Wash trough, the measured values of $\delta^{18}O$ indicate that the meteoric water responsible for deposition of the limestone was derived from more inland and/or relatively high elevations (e.g., Rozanski and others, 1993; Grootes, 1993).

Table 2. Isotopic Data, Hualapai Limestone

Map Location	Sample #[a]	Location (UTM)	$\delta^{13}C$ (PDB)[b]	$\delta^{18}O$ (PDB)[b]
1	97-141C	766180m E, 3998708m N	0.62	-10.22
2	97-152	766591m E, 3998357m N	1.40	-8.93
3	97-152A-1[c]	766591m E, 3998357m N	3.24	-9.93
	97-152A-2	766591m E, 3998357m N	2.96	-9.92
4	97-152B	766591m E, 3998357m N	3.10	-10.49
5	97-154A-1[e]	769505m E, 3996265m N	2.86	-10.81
	97-154A-2[f]	769505m E, 3996265m N	2.55	-14.44
6	97-155	769592m E, 3996080m N	2.92	-10.69
7	97-157A	769273m E, 3995171m N	3.65	-0.28
8	97-133F	769542m E, 3994880m N	3.07	-8.74
9	97-133D	770120m E, 3994325m N	3.05	-9.93
10	97-41B1	760739m E, 3993821m N	1.31	-11.60
	97-41B2	760739m E, 3993821m N	1.46	-11.56
11	97-140A	767060m E, 3992313m N	0.87	-12.23
12	97-140B	767048m E, 3992277m N	2.29	-9.81
13	97-140D	767036m E, 3992204m N	2.00	-12.48
14	97-142E	759298m E, 3992301m N	0.01	-12.15
15	97-142C	759216m E, 3992156m N	0.34	-12.26
16	97-142B	759216m E, 3992048m N	-0.23	-12.26
17	97-160-1	768611m E, 3990022m N	0.02	-11.27
	97-160-2[d]	768611m E, 3990022m N	-0.12	-10.29
18	97-160.5	769819m E, 3989386m N	0.27	-12.03

a All samples are of primary micrite unless otherwise noted.
b $\delta^{13}C$ and $\delta^{18}O$ values are relative to PDB standard, which is based on belemnites from the Cretaceous Peedee Formation, South Carolina (Faure, 1986).
c Fibrous cement (flowstone).
d Secondary cement within root/stem holes.
e Carbonate-cemented silt.
f Secondary sparry calcite.

Although the sample (#7, table 2) with the highest $\delta^{18}O$ value (i.e., the one exception) might be suggestive of a marine setting, it most likely represents evaporative carbonate formed in a marginal pool that was temporarily cut off from its water source, thus raising the $\delta^{18}O$ concentrations. Sparse interbeds of halite-rich siltstone within the limestone are compatible with the inferred evaporative environment. However, with only one of the 22 rock samples yielding a high $\delta^{18}O$ value, the data set indicates that evaporation was generally not a significant factor in producing the carbonate within the Grand Wash trough.

The composition and isotopic characteristics of the Hualapai Limestone in the both the Grapevine Wash area and Gregg Basin indicate deposition in one or more restricted warm, shallow, and quiet lakes fed by a relatively continuous source of fresh water in an evaporative climate (Wallace, 1999; Faulds and others, 2001c). In order to stay fresh, however, the lake or lakes probably had an outlet. The $\delta^{13}C$ and $\delta^{18}O$ data indicate that all of the sampled limestone is of nonmarine origin and that the water from which it precipitated was derived from relatively high elevations.

The age of the Hualapai Limestone in the Grand Wash trough is bracketed between ~11 and 7 Ma. As previously mentioned, a 10.94 Ma tephra is intercalated within the lowermost part of the Hualapai Limestone in the Grapevine Wash area. A tephra within the upper part of the limestone on Grapevine Mesa yielded a poorly defined $^{40}Ar/^{39}Ar$ age of 7.43±0.22 Ma, which should be considered a maximum eruptive age (M. Heizler, written commun., 1999). A tephra interbedded within the upper part of the Hualapai Limestone in the Temple Bar area ~25 km to the west of the Grand Wash trough yielded an $^{40}Ar/^{39}Ar$ age of 6.0 Ma on biotite (Spencer and others, 2001). The Hualapai Limestone in the Grand Wash trough may therefore be as young as ~6 Ma.

PLIOCENE-PLEISTOCENE DEPOSITS

As many as 16 mapped units postdate deposition of the Hualapai Limestone. Poorly sorted, subrounded to subangular clasts of local derivation, supported by a generally poorly consolidated silty and sandy matrix, indicate that several of these units are composed of sheetflood and debris flow deposits (Blatt and others, 1980) that accumulated on alluvial fans (e.g., QTf).

The late Tertiary stratigraphy at Sandy Point has important implications for the late Cenozoic paleogeographic evolution of the region. In ascending order, this sequence includes: 1) well-rounded, well-sorted, and clast-supported poorly to moderately indurated, commonly imbricated conglomerate, 2) a 4.4 Ma basalt flow (fig. 9), and 3) a capping sequence of unconsolidated well-sorted, clast-supported, rounded gravels and moderately to well-sorted, rounded to subrounded medium- to coarse-grained quartz arenite and siltstone with common medium-scale cross-bedding. The exposed section at Sandy Point lies ~100 m above the bed of the Colorado River (before the filling of Lake Mead). The upper unit of unconsolidated gravel and sand also crops out as thin erosional remnants (< 5 m thick) elsewhere near Lake Mead.

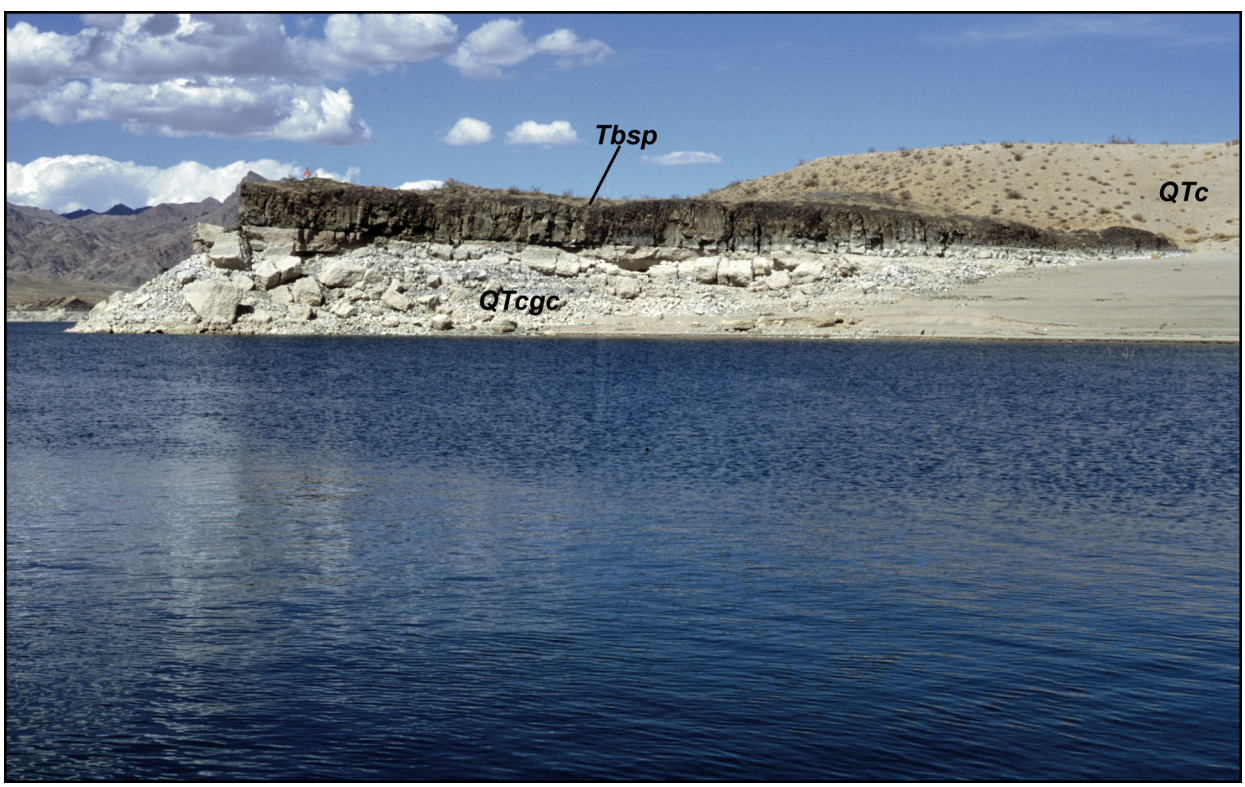

Figure 9. Looking northeast at 4.4 Ma basalt of Sandy Point (Tbsp), which is intercalated in Colorado River sediments (QTc and QTcgc).

The gravel and sand deposits are probably associated with a through-going Colorado River, as evidenced by: 1) the composition and texture of the deposits, including the well-developed sorting, clast-supported nature of the conglomerate and gravels, and well-developed pebble imbrication and cross bedding, all of which indicate a fluvial origin; 2) the pervasive well rounding and relatively large clast size (cobble size), which suggest a relatively vigorous fluvial system; and 3) a diverse suite of clast lithologies including fine-grained sandstone and quartzite, granite, gneiss, chert, limestone, and dolostone, much of which was derived from Paleozoic and Proterozoic strata in the Grand Canyon.

The intercalated basalt flow at Sandy Point yielded an $^{40}Ar/^{39}Ar$ groundmass concentrate age of 4.41±0.03 Ma (table 1; Faulds and others, 2001b). Previously reported K-Ar whole rock ages of this basalt were 3.79±0.46 Ma (Damon and others, 1978) and 2.6±0.9 Ma (Damon, 1965). The 4.4 Ma age of the basalt, which overlies well-rounded river gravels (fig. 9), suggests that the Colorado River had developed by at least 4.5 Ma. Accordingly, limestone deposition ended prior to 4.5 Ma.

STRUCTURAL FEATURES

The following structural features are described: 1) the northern Grand Wash fault zone; 2) a largely buried fault offsetting Paleozoic strata in the northernmost Lost Basin Range here referred to as the Meadview fault; 3) the right-stepping Wheeler Ridge and Lost Basin Range faults, including an associated hanging-wall syncline and relay ramp; and 4) folding within the limestone of the Grand Wash trough.

Northern Grand Wash Fault

The northern Grand Wash fault (cf., Faulds and others, 1997), which lies buried just east of the quadrangle, forms an abrupt boundary between the essentially unextended Colorado Plateau and highly extended northern Colorado River extensional corridor (figs. 1 and 2). To the south, the northern Grand Wash fault intersects the southern Grand Wash fault and links with the Cerbat Mountains fault (Faulds and others, 1997, 2001b). To the north, the northern Grand Wash fault merges with the Wheeler Ridge fault and continues north to the northern margin of the Grand Wash trough.

In the Lake Mead area, middle to late Miocene sedimentary rocks, including the Hualapai Limestone, onlap the subhorizontal Paleozoic strata of the Grand Wash Cliffs and thus cover the northern Grand Wash fault, obscuring its geometry. The general geometry of the northern Grand Wash fault can be inferred, however, from structures developed within its hanging wall and by association with previously documented fault geometries in the region. For example, a west-dipping, listric, normal fault geometry is inferred for the northern Grand Wash fault based on: 1) the sharp discordance in tilting between the footwall (Grand Wash Cliffs, subhorizontal) and hanging wall (Wheeler Ridge, 40–80°); 2) a rollover fold (cf., Hamblin, 1965; Groshong, 1989; Dula, 1991; Xiao and Suppe, 1992) developed in the moderately to steeply east-titled Paleozoic strata on Wheeler Ridge (Brady, 1998); 3) an upward decrease in eastward tilt from ~30° to 5° within the middle to late Miocene sedimentary rocks of the Grand Wash trough. Similar features and seismic reflection data document a listric geometry for the southern Grand Wash fault bounding the Hualapai basin to the south (Faulds and others, 1997).

In addition, the strike of the northern Grand Wash fault can be reasonably well inferred from the trend of the Grand Wash Cliffs and the average strike of tilted bedding on Wheeler Ridge and in the Grand Wash trough. On average, both Paleozoic and Tertiary strata strike north to north-northeast. Because tilting prior to Tertiary extension was minimal in the area, the northerly to north-northeasterly strikes probably reflect the approximate strike of the northern Grand Wash fault. The north-northeast trend of the Grand Wash Cliffs (fig. 1) supports this premise.

Meadview Fault

The poorly exposed northwest-striking Meadview fault truncates the ridge of steeply east-tilted Paleozoic strata on the south, juxtaposing these strata against the Proterozoic rocks of the northern Lost Basin Range. The north end of this fault may also cut the fanglomerate unit (Tcg) within the Gregg Basin. However, the nature of the Xgn-Tcg contact in this area is equivocal. Locally, Tcg appears to fill a steep channel cut into Xgn. Moreover, Tcg near the southern margin of the quadrangle is not cut by the Meadview fault. However, a fault is suggested by local brecciation of Xgn along the contact and an ~90° discordance between the strike of strata within Tcg and the Xgn-Tcg contact. The Meadview fault may link northward, beneath the onlapping strata of the Gregg Basin, with a steeply west-dipping “reverse” fault noted by Longwell (1936) on the west flank of Wheeler Ridge a few kilometers north of the quadrangle. Although poorly exposed, the trace of the Meadview fault indicates a steep dip.

The original dip of the Meadview fault is difficult to ascertain. The fault was apparently not active during the late stages of extension, as it does not cut the gently tilted Hualapai Limestone in the Gregg Basin nor the fanglomerate facies near Meadview. If active prior to or at the onset of extension, the Meadview fault may have originated at a moderate to gentle dip, possibly as a west-dipping Laramide thrust fault. Steep east-tilting of the northern Lost Basin Range would have rotated the Meadview fault to its present steep dip. The fault may have been reactivated as a normal fault as it was tilted to a moderate east dip. Alternatively, the Meadview fault may have simply originated as a moderately east-dipping normal fault during Miocene extension and before much of the fault-block tilting. It was then rotated to a steeper or possible westward dip during the last vestiges of movement on the northern Grand Wash fault. We currently favor the latter explanation, because it requires a simpler geologic history for the region and Laramide thrust faults have not been documented in the northern Colorado River extensional corridor.

Wheeler Ridge and Lost Basin Range Faults

A zone of northerly striking, west-dipping normal faults bounds Wheeler Ridge, Grapevine Mesa, and the Lost Basin Range on the west. The northern segment is referred to as the Wheeler Ridge fault, and the southern segment is termed the Lost Basin Range fault. The Wheeler Ridge fault links northward with the northern Grand Wash fault. The Lost Basin Range fault projects southward toward the southern Grand Wash fault (fig. 1). In contrast to most of the Grand Wash fault zone, however, the Wheeler Ridge and Lost Basin Range faults accommodated relatively young (late Miocene to Pliocene?) movement, as evidenced by ~275 m of offset of the uppermost part of the Hualapai Limestone (Lucchitta, 1966).

At the latitude of the South Cove Road, the Wheeler Ridge fault splays northward into the Sheep Canyon, South Cove, and Airport faults of Brady (1998). These three faults merge farther north to become the Wheeler Ridge fault again (fig. 4). To the south, at the latitude of the northernmost exposure of Early Proterozoic rocks forming the Lost Basin Range, the Wheeler Ridge fault breaks into several small splays and terminates. Displacement within the fault zone steps westward in this area to the Lost Basin Range fault. The Wheeler Ridge and Lost Basin Range faults do not overlap in a typical en echelon geometry, at least not at exposed levels.

The Lost Basin Range fault continues southward along the west flank of the Lost Basin Range juxtaposing late Miocene conglomerate and limestone in the hanging wall against Proterozoic rocks in the footwall. Older fans shed from the Lost Basin Range (QTf) appear to be cut by the fault, whereas younger fans (Qf) appear to onlap the fault. Because the ages of these fan deposits are poorly defined, the youngest episode of movement on the fault is not well constrained. Nonetheless, some Pleistocene displacement is possible.

The right-step between the Wheeler Ridge and Lost Basin Range faults forms a conspicuous relay ramp (cf., Larsen, 1988; Peacock and Sanderson, 1994), or synthetic accommodation zone (Faulds and Varga, 1998), that essentially connects the footwall of the southern segment with the hanging wall of the northern segment. The relay ramp is marked by a northwest-facing monocline of conglomerate (Tcg) and limestone (Thgb), which depositionally overlie a northwest-sloping surface of Proterozoic rock.

A west-dipping listric geometry is inferred for the Wheeler Ridge and Lost Basin Range faults. Eastward tilts of the limestone within the Gregg Basin slightly exceed that within the Grand Wash trough. Three point solutions yielded an average attitude of N3°W, 55°SW for the Wheeler Ridge fault, where it cuts sedimentary rocks in the Gregg Basin.

The Wheeler Ridge and Lost Basin Range faults probably accommodated a protracted episode of displacement. Restoration of the limestone beds to their original position juxtaposes the distinctive fine-grained basinal deposits in the Gregg Basin against the westerly-derived fanglomerate and megabreccia on the west flank of Grapevine Mesa. Earlier movement that predates deposition of the limestone facies but postdates the fanglomerate facies (i.e., between ~15 and 11 Ma) is therefore required on these faults.

Folding of Miocene Rocks

Two domains of folding in Miocene sedimentary rocks are found within the quadrangle. One is adjacent to the Wheeler Ridge and Lost Basin Range faults on the west, where a syncline, here referred to as the Gregg Basin syncline, trends roughly parallel to the faults (fig. 10). The second includes several north-south trending folds in the Grapevine Wash area in the southeast part of the quadrangle.

The Gregg Basin syncline is a large hanging-wall syncline that developed directly west of the Wheeler Ridge and Lost Basin Range faults (cross section B–B′) as a result of eastward tilting of the hanging-wall block and normal drag directly adjacent to the faults. The syncline trends from N10°W to N35°E. To the north, the syncline dies out as it crosses the latitude of South Cove Road. To the south, it swings to a northeasterly trend at the right step between the Wheeler Ridge and Lost Basin Range faults. Farther south, adjacent to the Lost Basin Range fault, it is buried by late Tertiary to Quaternary fans shed from the Lost Basin Range.

In the Grapevine Wash area in the southeast part of the quadrangle, the folding probably occurred contemporaneously with deposition of the Hualapai Limestone. More tightly folded lower limestone and interbedded sandstone-siltstone beds are capped by more gently tilted limestone. In many cases, the strike of the more gently folded uppermost beds differs from that of the underlying beds. Some individual siltstone interbeds are truncated in angular unconformities as they approach the hinges of the anticlines, whereas others gradually pinch out. The folding in this area is attributed to minor blind normal faulting in the subsurface. The more gentle tilting of capping limestone beds may be associated with local late-stage movement on splays of the northern Grand Wash fault and/or compaction-induced basin subsidence.

Timing of Extension and Folding

Stratigraphic and structural relations within the Meadview North Quadrangle and nearby areas bracket extension within the southern Grand Wash trough between ~16 and 11 Ma (Faulds and others, 2001b). The oldest exposed Tertiary units in the southern Grand Wash trough are middle Miocene tuffaceous rocks, fanglomerates, and megabreccia deposits. Appreciable tilt-fanning (~30° to 10°) within these units suggests synextensional deposition. The fanglomerates and megabreccias were derived primarily from the South Virgin Mountains to the west, as evidenced by abundant detritus of the 1.4 Ga Gold Butte Granite (Lucchitta, 1966, 1979). Beneath the fanglomerates at Wheeler Ridge, the 15.29±0.07 Ma nonwelded tuff rests directly on Cambrian rocks. It is tilted 30° east, about half that of the underlying Paleozoic strata. This suggests that tilting and extension, as well as

movement on the northern Grand Wash fault, began sometime before 15.3 Ma. On the basis of stratigraphic and structural relations to the northwest (e.g., Beard, 1993, 1996) and southwest (e.g., Faulds and others, 1995, 2001a, 2001b; Price and Faulds, 1999), we infer that extension in the southern Grand Wash trough began ~16 Ma. This is compatible with apatite fission-track ages indicating rapid unroofing of the Gold Butte block ~15.0±0.5 Ma (Fitzgerald and others, 1991) and $^{40}Ar/^{39}Ar$ data suggesting appreciable extension in the northern White Hills ~15 Ma (Duebendorfer and Sharp, 1998). Overlying the fanglomerate unit are the gently tilted ~13 to 11 Ma sandstone-siltstone deposit and ~11 to 6 Ma Hualapai Limestone. Minor tilting (~5°) of the sandstone-siltstone unit indicates that displacement on the northern Grand Wash fault had largely abated by about 13 Ma. Displacement on the northern Grand Wash fault probably ended shortly after 11 Ma, as the middle to upper parts of the Hualapai Limestone onlap the fault.

The timing of movement on the Wheeler Ridge and Lost Basin Range faults can also be roughly constrained. Deformation began prior to the onset of limestone deposition, as evidenced by the distribution and composition of both the limestone and underlying sandstone-siltstone facies. Latest movement clearly postdates deposition of the uppermost ~6 Ma part of the limestone, because the uppermost beds are offset by ~275 m. The 4.4-Ma basalt of Sandy Point was probably deposited after most of the movement on the fault, as appreciable offset of Colorado River sediments has not been documented in the area. Thus, much of the movement on the Wheeler Ridge and Lost Basin Range faults probably occurred between ~13 and 4.4 Ma.

The folding in the southeast part of the quadrangle disrupts the upper part of the limestone section but does not affect overlying late Tertiary-Quaternary fan deposits (QTf). Because an unfolded, gently-tilted limestone bed does overlie the more tightly folded layers, the timing of folding is constrained by the 11 to 6 Ma age of the Hualapai Limestone.

On the basis of the above relations, major extension in the vicinity of the Grand Wash trough occurred between ~16 and 4.4 Ma. Most of the movement on the northern Grand Wash fault took place ~16 to 11 Ma, whereas the Wheeler Ridge and Lost Basin Range faults largely accommodated motion between ~13 and 4.4 Ma. However, the Wheeler Ridge fault zone has also accommodated some Quaternary movement (Lucchitta, 1966; S. Beard, personal commun., 1997). The general time frame for extension in the vicinity of the Grand Wash trough overlaps with the 16 to 8 Ma episode documented in the southern White Hills to the south (Price, 1997; Price and Faulds, 1999) and 15.2 to 11 Ma episode recognized in the northern White Hills to the west (Duebendorfer and Sharp, 1998).

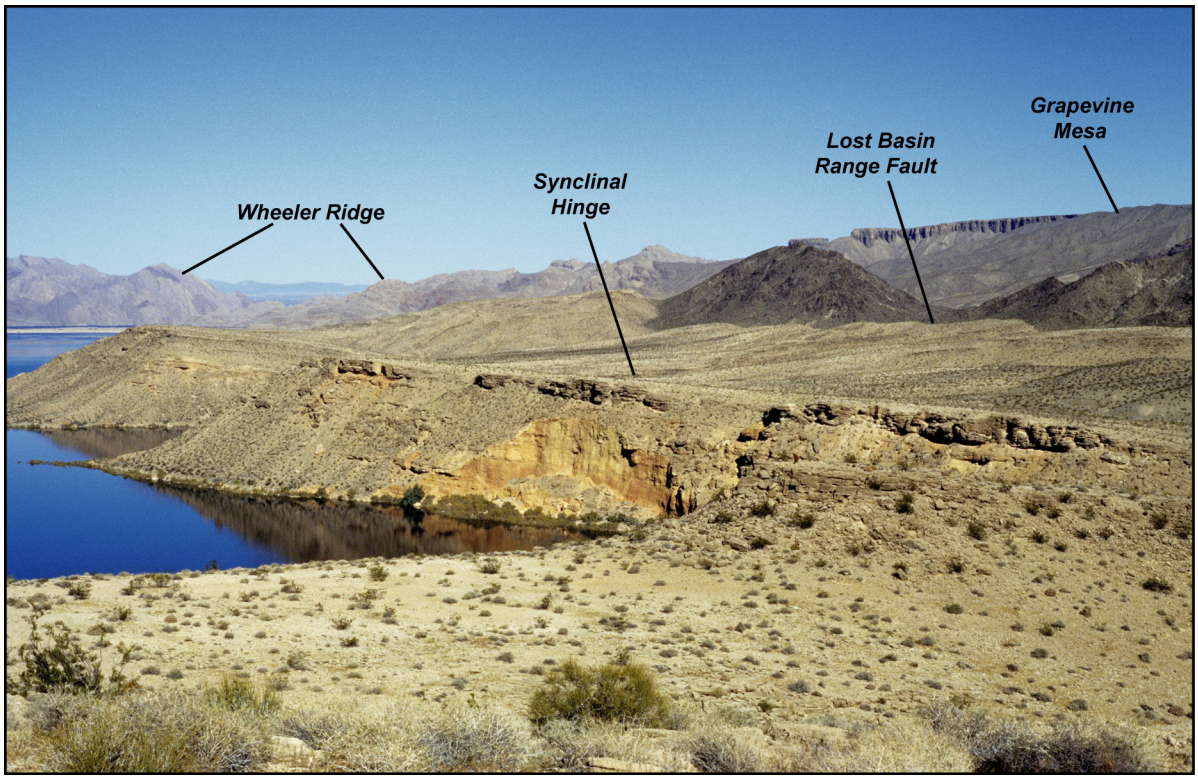

Figure 10. Gregg Basin syncline, looking northeast from southwest corner of the quadrangle. This syncline results from east-tilting of the Gregg Basin half graben and normal drag along the west-dipping Wheeler Ridge and Lost Basin Range faults. Thus, it is extensional in origin.

GEOMORPHIC FEATURES

The most conspicuous geomorphic feature within the Meadview North Quadrangle is Grapevine Mesa (fig. 3). Data from two wells from the Meadview area on Grapevine Mesa were incorporated into the geologic mapping (table 3 and fig. 4). Although highly dissected by erosion and locally deformed by faults and folds, the present upper surface of this relatively flat-lying mesa is primarily developed on the uppermost part of the Hualapai Limestone. Thus, this surface essentially corresponds to a lake bottom that immediately predates arrival of the Colorado River. Lacustrine deposits within the Lake Mead region are as young as ~5.5 Ma (e.g., Castor and Faulds, 2001). Additionally, the 4.4 Ma basalt flow at Sandy Point overlies Colorado River gravels. These relations suggest that the Colorado River entered the region between ~5.5 and 4.4 Ma (Faulds and others, 2002a). Thus, the upper surface of Grapevine Mesa is probably about 5–6 Ma. The lack of any fluvial sediment either intercalated within or above the Hualapai Limestone at Grapevine Mesa

Table 3. Descriptions of Cuttings from Meadview Wells

D1

Description	Thickness (m)	Total depth below surface (m)*
Sand and gravel	9.1	9.1
Cemented gravel	9.1	18.3
Cemented gravel	12.2	30.5
Cemented sand	15.2	45.7
Cemented gravel	12.2	57.9
Cemented gravel	7.6	65.5
Cemented gravel	12.2	77.7
Cemented gravel	18.3	96.0
Brown cemented gravel	18.3	114.3
Brown cemented gravel	10.7	125.0
Brown cemented gravel	10.7	135.7
Brown cemented gravel	1.5	137.2
Gravel, sand, and quartz	6.1	143.3
Sand, gravel, and quartz	6.1	149.4
Cemented gravel with lime shells	7.6	157.0
Limestone and quartz	3.0	160.0
Gray sand and water	1.2	161.2
Limestone gravel	4.9	166.1
White limestone	3.0	169.1
Cemented gravel	4.6	173.7
Cemented gravel	6.1	179.8

D2

Description	Thickness (m)	Total depth below surface (m)*
Brown clay with sand and gravel	18.3	18.3
Gravel-sand cemented	18.3	36.6
Boulders	0.6	37.2
Cemented gravel and sand	14.6	51.8
Boulders	0.6	52.4
Cemented gravel	13.1	65.5
Granitic boulder	0.9	66.4
Brown clay with gravel and sand	21.9	88.3
Coarse gravel	1.5	89.8
Cemented gravel and sand	4.6	94.4
Cemented gravel	5.8	100.2
Granitic boulders	0.9	101.1
Cemented gravel	31.7	132.8
Brown sand, clay, and gravel	29.0	161.8
Cemented gravel	7.3	169.1
Hard cemented gravel	15.2	184.3
Granitic boulders	>1.2	185.5

Descriptions of cuttings from two wells (D1 and D2) located at 36°00’34”N, 114°04’04”W and 35°59’43”N, 114°04’25”W, respectively (see Fig. 4 for locations of D1 and D2). D2 is just south of quadrangle. Drilling and descriptions were performed by Patrick H. Thompson (Las Vegas, Nevada) in 1971, for the Rivcor Corporation (Meadview, Arizona) and Landex (Phoenix, Arizona). Data were obtained from the Joshua Valley Utility Company and are known as well numbers B(30-17)11-1 and B(30-17)14-1 (written commun., 1998).
* refers to surface elevations of 889 and 933 m above sea level for D1 and D2, respectively.

further implies that once the Colorado River arrived, the lake drained abruptly and canyon cutting ensued immediately. More than 600 m of subsequent dissection by the Colorado River and its tributaries have beautifully exposed Tertiary and Paleozoic strata within the Grand Wash trough.

CONCLUSIONS

The stratigraphic and structural framework of the Meadview North Quadrangle affords the following interpretations:

1) Prior to deposition of the fanglomerate facies, probably during middle Miocene time, the east(?)-trending Wheeler Ridge paleocanyon was carved into the Paleozoic strata of Wheeler Ridge.

2) The fanglomerate facies, which ranges from ~15 to 11 Ma, was primarily derived from crystalline terranes (South Virgin Mountains and Lost Basin Range) to the west and southwest of the Grand Wash trough (e.g., Lucchitta, 1966). The imposing fault-line escarpment of the Grand Wash Cliffs contributed relatively little detritus into these basins. Rock-avalanche deposits intercalated in the fanglomerate facies were also derived from source areas mainly to the west and southwest.

3) Sandstone-siltstone facies: The sandstone-siltstone facies, which underlies the Hualapai Limestone, primarily accumulated within a continental playa, as evidenced by primary sedimentary structures and intercalated deposits of primary gypsum. The composition and reddish color of this facies suggest at least partial derivation from Permian redbeds on the Colorado Plateau and/or to the north of the Grand Wash trough.

4) Limestone facies: The Hualapai Limestone is nonmarine, as evidenced by petrographic features, fossil assemblages, and $\delta^{13}C$–$\delta^{18}O$ isotopic data. The limestone accumulated primarily in a lacustrine environment, the source waters of which emanated from relatively high elevations. The $\delta^{18}O$ isotopic data suggest that the lake(s) generally had an outlet. Evaporative episodes did occur but were brief and infrequent. The age of the limestone is bracketed between ~11 and 6 Ma.

5) Major extension within the Grand Wash trough is roughly bracketed between 16 and 4.4 Ma. Extension was largely accommodated on a system of west-dipping, listric normal faults.

6) Major faults within the area include the concealed northern Grand Wash fault and locally exposed Wheeler Ridge and Lost Basin Range faults. The distribution of the sandstone-siltstone facies suggests that the fault zones were active prior to ~11 Ma. However, the Hualapai Limestone onlaps the northern Grand Wash fault. In contrast, the Wheeler Ridge fault accommodates 275 m of offset of the limestone. These and regional relations indicate that the northern Grand Wash fault was active primarily between 16 and 11 Ma, whereas the Wheeler Ridge-Lost Basin Range fault system was active mainly between ~13 and 4.4 Ma.

7) A north-facing monoclinal relay ramp (e.g., Larsen, 1988) links the tips of the Wheeler Ridge and Lost Basin Range faults.

8) The 4.4 Ma age of the basalt of Sandy Point places an important constraint on the age of the Colorado River, as the basalt overlies Colorado River gravels. Thus, the Colorado River must have been established in the eastern Lake Mead area by at least 4.4 Ma.

9) Sometime between ~5.5 and 4.4 Ma, the through-going Colorado River developed in the Lake Mead area, which probably coincided with significant down-cutting in the Grand Canyon.

10) On the basis of a) significant offset on the northern Grand Wash fault between ~16 and 13 Ma and attendant development of the sharp topographic boundary between the Colorado Plateau and Basin and Range province, b) the lacustrine origin of the 11 to 6 Ma Hualapai Limestone, c) apparent high-elevation source waters for the Hualapai lake(s), and d) possible derivation of some of the sandstone-siltstone facies from the Colorado Plateau, we suggest that a precursor to the Colorado River (i.e., west-flowing stream(s) eroding headward into the Colorado Plateau) began developing and feeding the limestone lakes by ~11 Ma, probably during or immediately following the major phase of extension (16–11 Ma) in the northern Colorado River extensional corridor. Some excavation of the lower Grand Canyon may have begun during this time.

11) Grapevine Mesa (fig. 3) essentially represents the ancient lake bottom of the Hualapai lake immediately prior to arrival of the Colorado River. The lack of any fluvial sediment either intercalated within or resting above the Hualapai Limestone at Grapevine Mesa suggests a rapid transition from lacustrine to fluvial deposition that may correlate with an abrupt arrival of the Colorado River and swift draining of the lake.

ACKNOWLEDGMENTS

Field work was supported by an EDMAP grant from the U.S. Geological Survey (Cooperative agreement #1434-HQ-97-AG-07146) and National Science Foundation grant EAR99-10977 awarded to Faulds. The U.S. Geological Survey also provided a field vehicle and funds for cartographic work for which we thank Gary Dixon and Peter Rowley. The National Park Service at Lake Mead National Recreation Area kindly provided boat access into relatively inaccessible areas. We also thank Keith Howard, Jon

Spencer, and Sue Beard for constructive reviews that greatly improved the map and text. Fruitful discussions with Luis Gonzalez, Ivo Lucchitta, George Billingsley, and Joel Pederson were also very helpful.

REFERENCES

Albin, A.A., and Karlstrom, K.E., 1991, Orthogonal Proterozoic fabrics in northwestern Arizona: Multiple orogenic events or progressive deformation during continental assembly, *in* Karlstrom, K.E., ed., Proterozoic Geology and Ore Deposits of Arizona: Arizona Geological Society Digest, v. 19, p. 67–84.

Anderson, R.E., 1973, Large-magnitude late Tertiary strike-slip faulting north of Lake Mead, Nevada: U.S. Geological Survey Professional Paper 794, 18 p.

Anderson, R.E., Longwell, C.R., Armstrong, R.L., and Marvin, R.F., 1972, Significance of K-Ar ages of Tertiary rocks from the Lake Mead region, Nevada-Arizona: Geological Society of America Bulletin, v. 83, p. 273–288.

Beard, L.S., 1993, Tertiary stratigraphy of the South Virgin Mountains, southeast Nevada, and the Grand Wash trough, northwest Arizona, *in* Sherrod, D.R., and Nielson, J.E., eds., Tertiary stratigraphy of highly extended terranes, California, Arizona, and Nevada: U.S. Geological Survey Bulletin 2053, p. 29–32.

Beard, L.S., 1996, Paleogeography of the Horse Spring Formation in relation to the Lake Mead fault system, Virgin Mountains, Nevada and Arizona, *in* Beratan, K.K., ed., Reconstructing the history of Basin and Range extension using sedimentology and stratigraphy: Geological Society of America Special Paper 303, p. 27–59.

Billingsley, G.H., Beard, L.S., Priest, S.S., Wellmeyer, J.L., and Block, D.L., 2004, Geologic map of the lower Grand Wash Cliffs and vicinity, Mohave County, northwestern Arizona: U.S. Geological Survey Miscellaneous Field Studies Map MF-2427, scale 1:31,680.

Blacet, P.M., 1975, Preliminary geologic map of the Garnet Mountain quadrangle, Mohave County, Arizona: U.S. Geological Survey Open-File Map 75-93, scale 1:62,500.

Blair, W.N., 1978, Gulf of California in the Lake Mead area of Arizona and Nevada during late Miocene time: American Association of Petroleum Geologists Bulletin, v. 62, p. 1159–1170.

Blair, W.N., and Armstrong, A.K., 1979, Hualapai Limestone Member of the Muddy Creek Formation: The youngest deposit predating the Grand Canyon, southeastern Nevada and northwestern Arizona: U.S. Geological Survey Professional Paper 1111, 14 p.

Blatt, H., Middleton, G., and Murray, R., 1980, Origin of sedimentary rocks: Prentice-Hall, Englewood Cliffs, New Jersey, 782 p.

Bohannon, R.G., 1984, Nonmarine sedimentary rocks of Tertiary age in the Lake Mead region, southeastern Nevada and northwestern Arizona: U.S. Geological Survey Professional Paper 1259, 72 p.

Bradbury, J.P., and Blair, W.N., 1979, Paleoecology of the upper Miocene Hualapai Limestone Member of the Muddy Creek Formation, northwest Arizona, in Newman, G.W., and Goode, H.D., eds., Basin and Range symposium and Great Basin field conference: Rocky Mountain Association of Geologists Guidebook, Denver, p. 292–303.

Brady, R.J., 1998, The geology of the Gold Butte breakaway zone and the mechanical evolution of normal fault systems [Ph.D. dissertation]: California Institute of Technology, Pasadena, 188 p.

Brady, R.J., Wernicke, B., and Fryxell, J., 2000, Kinematic evolution of a large-offset continental normal fault system, South Virgin Mountains, Nevada: Geological Society of America Bulletin, v. 112, no. 9, p. 1375–1397.

Buising, A.V., 1990, The Bouse Formation and bracketing units, southeastern California and western Arizona: Implications for the evolution of the proto-Gulf of California and the lower Colorado River: Journal of Geophysical Research, v. 95, p. 20, 111–20, 132.

Castor, S.B., and Faulds, J.E., 2001, Post-6-Ma limestone along the southeast part of the Las Vegas Valley shear zone, southern Nevada, *in* Young, R.A., and Spamer, E.E., eds., The Colorado River: Origin and evolution: Grand Canyon, Arizona, Grand Canyon Association Monograph 12, p. 77–80.

Damon, P.E., 1965, Correlation and chronology of ore deposits and volcanic rocks: Annual Progress Report to U.S. Atomic Energy Commission C00-689-50, Geochronology Laboratories, University of Arizona, 60 p.

Damon, P.E., Shafiqullah, M., and Scarborough, R.B., 1978, Revised chronology for critical stages in the evolution of the lower Colorado River: Geological Society of America Abstracts with Programs, v. 10, no. 3, p. 101–102.

Drever, J.I., 1997, The geochemistry of natural waters: Prentice-Hall, Englewood Cliffs, New Jersey, 436 p.

Duebendorfer, E.M., and Wallin, E.T., 1991, Basin development and syntectonic sedimentation associated with kinematically coupled strike-slip and detachment faulting, southern Nevada: Geology, v. 19, p. 87–90.

Duebendorfer, E.M., and Simpson, D.A., 1994, Kinematics and timing of Tertiary extension in the western Lake Mead region, Nevada: Geological Society of America Bulletin, v. 106, p. 1057–1073.

Duebendorfer, E.M., and Sharp, W.D., 1998, Variation in displacement along strike of the South Virgin-White Hills detachment fault: Perspective from the northern White Hills, northwestern Arizona: Geological Society of America Bulletin, v. 110, p. 1574–1589.

Duebendorfer, E.M., Beard, L.S., and Smith, E.I., 1998, Restoration of Tertiary deformation in the Lake Mead region, southern Nevada: The role of strike-slip transfer faults, *in* Faulds, J.E., and Stewart, J.H., eds.,

Accommodation zones and transfer zones: The regional segmentation of the Basin and Range province: Geological Society of America Special Paper 323, p. 127–148.

Dula, W.F., 1991, Geometric models of listric normal faults and rollover folds: American Association of Petroleum Geologists Bulletin, v. 75, p. 1609–1625.

Faulds, J.E., 1993, Miocene stratigraphy of the central Black Mountains, northwestern Arizona: Variations across a major accommodation zone, *in* Sherrod, D.R., and Nielson, J.E., eds., Tertiary stratigraphy of highly extended terranes, California, Arizona, and Nevada: U.S. Geological Survey Bulletin, v. 2053, p. 37–44.

Faulds, J.E., Geissman, J.W., and Mawer, C.K., 1990, Structural development of a major extensional accommodation zone in the Basin and Range province, northwestern Arizona and southern Nevada, *in* Wernicke, B., ed., Basin and Range extensional tectonics near the latitude of Las Vegas, Nevada: Geological Society of America Memoir 176, p. 37–76.

Faulds, J.E., Geissman, J.W., and Shafiqullah, M., 1992, Implications of paleomagnetic data on Miocene extension near a major accommodation zone in the Basin and Range province, northwestern Arizona and southern Nevada: Tectonics, v. 11, p. 204–227.

Faulds, J.E., Feuerbach, D.L., Reagan, M.K., Metcalf, R.V., Gans, P., and Walker, J.D., 1995, The Mount Perkins block, northwestern Arizona: An exposed cross section of an evolving preextensional to synextensional magmatic system: Journal of Geophysical Research, v. 100, p. 15,249–15,266.

Faulds, J.E., Schreiber, B.C., Reynolds, S.J., Gonzalez, L., and Okaya, D., 1997, Origin and paleogeography of an immense, nonmarine Miocene salt deposit in the Basin and Range (western USA): Journal of Geology, v. 105, p. 17–36.

Faulds, J.E., and Varga, R., 1998, The role of accommodation zones and transfer zones in the regional segmentation of extended terranes: Geological Society of America Special Paper 323, p. 1–46.

Faulds, J.E., Smith, E.I., and Gans, P., 1999, Spatial and temporal patterns of magmatism and extension in the northern Colorado River extensional corridor, Nevada and Arizona: A preliminary report: Nevada Petroleum Society Guidebook, p. 171–183.

Faulds, J.E., Feuerbach, D.L., Miller, C.F., and Smith, E.I., 2001a, Cenozoic evolution of the northern Colorado River extensional corridor, southern Nevada and northwest Arizona: Pacific Section of the American Association of Petroleum Geologists Publication GB 78 (also Utah Geological Association Publication 30), p. 239–272.

Faulds, J.E., Price, L.M., and Wallace, M.A., 2001b, Pre-Colorado River paleogeography and extension along the Colorado Plateau-Basin and Range boundary, northwest Arizona, *in* Young, R.A., and Spamer, E.E., eds., The Colorado River: Origin and evolution: Grand Canyon, Arizona, Grand Canyon Association Monograph 12, p. 93–99.

Faulds, J.E., Wallace, M.A., Gonzalez, L.A., and Heizler, M., 2001c, Depositional environment and paleogeographic implications of the late Miocene Hualapai Limestone, northwest Arizona and southern Nevada, *in* Young, R.A., and Spamer, E.E., eds., The Colorado River: Origin and evolution: Grand Canyon, Arizona, Grand Canyon Association Monograph 12, p. 81–87.

Faulds, J.E., Gonzalez, L.A., Perkins, M.E., House, P.K., Pearthree, P.A., Castor, S.B., and Patchett, P.J., 2002a, Late Miocene-early Pliocene transition from lacustrine to fluvial deposition: Inception of the lower Colorado River in southern Nevada and northwest Arizona: Geological Society of America Abstracts with Programs, v. 34, no. 4, p. 60.

Faulds, J.E., Olson, E.L., Harlan, S.S., and McIntosh, W.C., 2002b, Miocene extension and fault-related folding in the Highland Range, southern Nevada: A three-dimensional perspective: Journal of Structural Geology, v. 24, p. 861–886.

Faure, G., 1986, Principles of isotope geology: John Wiley & Sons, New York, 557 p.

Fitzgerald, P.G., Fryxell, J.E., and Wernicke, B.P., 1991, Miocene crustal extension and uplift in southeastern Nevada: Constraints from fission track analysis: Geology, v. 19, p. 1013–1016.

Fryxell, J.E., Salton, G.S., Selverstone, J.E., and Wernicke, B., 1992, Gold Butte crustal section, South Virgin Mountains, Nevada: Tectonics, v. 11, p. 1099–1120.

Gans, P.B., and Bohrson, W.A., 1998, Suppression of volcanism during rapid extension in the Basin and Range province, United States: Science, v. 279, p. 66–68.

Grootes, P.M., 1993, Interpreting continental oxygen isotope records, *in* Stewart, P.K., Lohmann, K.C., McKenzie, J., and Savin, S., eds., Climate change in continental isotope records: Geophysical Monograph 78, p. 37–46.

Groshong, R.J., Jr., 1989, Half-graben structures: Balanced models of extensional fault-bend folds: Geological Society of America Bulletin, v. 101, p. 96–105.

Halfman, J.D., Johnson, T.C., Showers, W.J., and Lister, G.S., 1989, Authigenic low-Mg calcite in Lake Turkana, Kenya: Journal of African Earth Sciences, v. 8, p. 533–540.

Hamblin, W.K., 1965, Origin of "reverse drag" on the downthrown side of normal faults: Geological Society of America Bulletin, v. 76, p. 1145–1164.

Harlan, S.S., Duebendorfer, E.M., and Deibert, J.E., 1998, $^{40}Ar/^{39}Ar$ age determinations from Miocene volcanic rocks in the western Lake Mead area and southern Las Vegas Range, Nevada: Canadian Journal of Earth Sciences, v. 35, p. 495–503.

Harrison, J.V., and Falcon, N.L., 1937, An ancient landslip at Saidmarreh in southwestern Iran: Geographical Journal, v. 89, p. 42–47.

Heckel, P.H., 1972, Recognition of ancient shallow marine environments, *in* Rigby, J.K., and Hamblin, W.K., eds., Recognition of ancient sedimentary environments, Society of Economic Paleontologists and Mineralogists Special Publication, v. 16, p. 226–286.

Hillaire-Marcel, C., and Casanova, J., 1987, Isotopic hydrology and paleohydrology of the Magadi (Kenya)-Natron (Tanzania) basin during the late Quaternary: Paleogeography, Paleoclimatology, Paleoecology, v. 58, p. 155–181.

Howard, K.A., and John, B.E., 1987, Crustal extension along a rooted system of imbricate low-angle faults, Colorado River extensional corridor, California and Arizona, *in* Coward, M.P., Dewey, J.F., and Hancock, P.L., eds., Continental extensional tectonics: Geological Society of London Special Publication 28, p. 299–311.

Howard, K.A., Hook, S.J., Phelps, G.A., and Block, D.L., 2003, Geologic map of the Hiller Mountains Quadrangle, Clark County, Nevada, and Mohave County, Arizona: Nevada Bureau of Mines and Geology Map 137, scale 1:24,000, with accompanying text.

Karlstrom, K.E., and Bowring, S.A., 1991, Styles and timing of Early Proterozoic deformation in Arizona: Constraints on tectonic models, *in* Karlstrom, K.E., ed., Proterozoic geology and ore deposits of Arizona: Arizona Geological Society Digest, v. 19, p. 1–10.

Larsen, P.H., 1988, Relay structures in a Lower Permian basement-involved extensional system, East Greenland: Journal of Structural Geology, v. 10, p. 3–8.

Lee, W.T., 1908, Geologic reconnaissance of a part of western Arizona: U.S. Geological Survey Bulletin 352, 96 p.

Longwell, C.R., 1928, Geology of the Muddy Mountains, Nevada: U.S. Geological Survey Bulletin 798, 152 p.

Longwell, C.R., 1936, Geology of the Boulder Reservoir floor, Arizona-Nevada: Geological Society of America Bulletin, v. 47, p. 1393–1476.

Lucchitta, I., 1966, Cenozoic Geology of the upper Lake Mead area adjacent to the Grand Wash Cliffs, Arizona [Ph.D. thesis]: Pennsylvania State University, University Park, 218 p.

Lucchitta, I., 1979, Late Cenozoic uplift of the southwestern Colorado Plateau and adjacent lower Colorado River region: Tectonophysics, v. 61, p. 63–95.

Lucchitta, I., 1989, History of the Grand Canyon and of the Colorado River in Arizona: Arizona Geological Society Digest, v. 17, p. 701–715.

Lucchitta, I., 1998, The upper Miocene Bouse Formation as an indicator for late Cenozoic uplift of the Colorado Plateau: Geological Society of America Abstracts with Programs, v. 30, p. 14.

Lucchitta, I., Beard, L.S., and Rieck, H.J., 1986, Geologic map of the Pigeon Canyon, Nevershine Mesa, and Snap Point Wilderness Study Areas, Mohave County, Arizona: U.S. Geological Survey Miscellaneous Field Studies Map 1860-B, scale 1:50,000.

Lucchitta, I., and Young, R.A., 1986, Structure and geomorphic character of western Colorado Plateau in the Grand Canyon-Lake Mead region, *in* Nations, J.D., Conway, C.M., and Swann G.A., eds., Geology of central and northern Arizona: Geological Society of America, Rocky Mountain Section Guidebook, Flagstaff, Northern Arizona University, p. 159–176.

McKee, E.D., and McKee, E.H., 1972, Pliocene uplift of the Grand Canyon region: Time of drainage adjustment: Geological Society of America Bulletin, v. 83, p. 1923–1932.

McKenzie, J.A., 1985, Carbon isotopes and productivity in the lacustrine and marine environment, *in* Stumm, W., ed., Chemical processes in lakes: John Wiley and Sons, New York, p. 99–118.

Metzger, D.G., 1968, The Bouse Formation (Pliocene) of the Parker-Blythe-Cibola area, Arizona and California: U.S. Geological Survey Professional Paper 600-D, p. 126–136.

Nilsen, T.H., and Moore, T.E., 1984, Bibliography of alluvial-fan deposits: Geo Abstracts Bibliography, v. 14, 96 p.

Peacock, D.C.P., and Sanderson, D.J., 1994, Geometry and development of relay ramps in normal fault systems: American Association of Petroleum Geologists Bulletin, v. 78, p. 147–165.

Peirce, H.W., 1985, Arizona's backbone: The transition zone: Arizona Bureau of Geology and Mineral Technology, Fieldnotes, v. 15, p. 1–6.

Perkins, M.E., Brown, F.H., Nash, W.P., McIntosh, W., and Williams, S.K., 1998, Sequence, age, and source of silicic fallout tuffs in middle to late Miocene basins of the northern Basin and Range province: Geological Society of America Bulletin, v. 110, p. 344–360.

Perkins, M.E., and Nash, W.P., 2002, Explosive silicic volcanism of the Yellowstone hotspot: The ash fall tuff record: Geological Society of America Bulletin, v. 114, no. 3, p. 367–381.

Perkins, M.E., Nash, W.P., Brown, F.H., and Fleck, R.J., 1995, Fallout tuffs of Trapper Creek, Idaho-A record of Miocene explosive volcanism in the Snake River plain volcanic province: Geological Society of America Bulletin, v. 107, p. 1484–1506.

Pierson, T.C., and Costa, J.E., 1987, A rheologic classification of subaerial sediment-water flows: Geological Society of America Reviews in Engineering Geology, v. 7, p. 1–12.

Price, L.M., 1997, The geometry and evolution of a major segment of the Grand Wash fault zone and associated growth-fault basins, southern White Hills, northwestern Arizona [M.S. thesis]: University of Iowa, Iowa City, 148 p.

Price, L.M., and Faulds, J.E., 1999, Structural development of a major segment of the Colorado Plateau-Basin and Range boundary, southern White Hills, Arizona: Nevada Petroleum Society Guidebook, p. 139–170.

Rowland, S.M., Parolini, J.R., Eschner, E., McAllister, A.J., and Rice, J.A., 1990, Sedimentologic and stratigraphic constraints on the Neogene translation and rotation of the Frenchman Mountain structural block, Clark County, Nevada, *in* Wernicke, B. P., ed., Basin and Range extensional tectonics near the latitude of Las Vegas, Nevada: Geological Society of America Memoir 176, p. 99–122.

Rozanski, K., Araguás-Araguás, L., and Gonfiantini, R., 1993, Isotopic patterns in modern global precipitation, *in* Stewart, P.K., Lohmann, K.C., McKenzie, J., and Savin, S., eds., Climate change in continental isotope records: Geophysical Monograph 78, p. 1–36.

Sheppard, S.M.F., Nielsen, R.L., and Taylor, H.P., 1969, Oxygen and hydrogen isotope ratios of clay minerals from porphyry copper deposits: Economic Geology, v. 64, p. 755–777.

Silver, L.T., Bickford, M.E., Van Schmus, W.R., Anderson, J.L., Anderson, T.H., and Medaris, L.G., Jr., 1977, The 1.4–1.5 b.y. transcontinental anorogenic plutonic perforation of North America: Geological Society of America Abstracts with Programs, v. 9, p. 1176–1177.

Smith, P.B., 1970, New evidence for a Pliocene marine embayment along the lower Colorado River area, California and Arizona: Geological Society of America Bulletin, v. 81, p. 1411–1420.

Spencer, J.E., and Patchett, P.J., 1997, Sr isotope evidence for a lacustrine origin for the upper Miocene to Pliocene Bouse Formation, lower Colorado River trough, and implications for timing of Colorado Plateau uplift: Geological Society of America Bulletin, v. 109, p. 767–778.

Spencer, J.E., Peters, L., McIntosh, W.C., and Patchett, P.J., 2001, $^{40}Ar/^{39}Ar$ geochronology of the Hualapai Limestone and Bouse Formation and implications for the age of the lower Colorado River, *in* Young, R.A., and Spamer, E.E., eds., The Colorado River: Origin and evolution: Grand Canyon, Arizona, Grand Canyon Association Monograph 12, p.89–92.

Spencer, R.J., Baedecker, M.J., Eugster, H.P., Forester, R.M., Goldhaber, M.B., Jones, B.F., Kelts, K., McKenzie, J., Madsen, D.B., Rettig, S.L., Rubin, M., and Bowser, C.J., 1984, Great Salt Lake, and precursors, Utah—The last 30,000 years: Contributions to Mineralogy and Petrology, v. 86, p. 321–334.

Stiller, M., and Hutchinson, G.E., 1980, The waters of Merom, a study of Lake Huleh, part 1—Stable isotopic composition of carbonates of a 54 m core, paleoclimatic and paleotrophic implications: Archiv für Hydrobiologie, v. 89, p. 275–302.

Stuiver, M., 1970, Oxygen and carbon isotope ratios of fresh-water carbonates as climatic indicators: Journal of Geophysical Research, v. 75, p. 5247–5257.

Talbot, M.R., and Kelts, K., 1990, Paleolimnological signatures from carbon and oxygen isotopic ratios in carbonates from organic carbon-rich lacustrine sediments, *in* Katz, B.J., ed., Lacustrine Basin Exploration: Case studies and modern analogs: American Association of Petroleum Geologists Memoir 50, p. 99–112.

Tenzer, G.E., Meyers, P.A., and Knoop, P., 1997, Sources and distribution of organic and carbonate carbon in surface sediments of Pyramid Lake, Nevada: Journal of Sedimentary Research, v. 67, p. 884–890.

Theodore, T.G., Blair, W.N., and Thomas, J.T., 1987, Geology and gold mineralization of the Gold basin-Lost basin mining districts, Mohave County, Arizona: U.S. Geological Survey Professional Paper 1361, 167 p.

Volborth, A., 1962, Rapakivi-type granites in the Precambrian complex of Gold Butte, Clark County, Nevada: Geological Society of America Bulletin, v. 73, p. 813–832.

Wallace, M.A., 1999, Cenozoic stratigraphic and structural framework of the southern Grand Wash trough, northwestern Arizona: Paleogeographic implications [M.S. thesis]: University of Iowa, Iowa City, 119 p.

Wasserburg, G.J., and Lanphere, M.A., 1965, Age determinations in the Precambrian of Arizona and Nevada: Geological Society of America Bulletin, v. 76, p. 735–758.

Xiao, H., and Suppe, J., 1992, Origin of rollover: American Association of Petroleum Geologists Bulletin, v. 76, p. 509–529.

Yarnold, J.C., and Lombard, J.P., 1989, A facies model for large rock-avalanche deposits formed in dry climates, *in* Colburn, I.P., Abbot, P.L., and Minch, J., eds., Conglomerates in basin analysis: A symposium dedicated to A.O. Woodford: Pacific Section, Society of Economic Petrologists and Mineralogists, v. 62, p. 9–31.

Young, R.A., 1970, Geomorphological implications of pre-Colorado tributary drainage in the western Grand Canyon region: Plateau, v. 42, no. 3, p. 107–117.

Young, R.A., 1979, Laramide deformation, erosion and plutonism along the southwestern margin of the Colorado Plateau: Tectonophysics, v. 61, p. 25–47.